Carricondo-Antón, JM.; Jiménez Bello, MA.; Manzano Juarez, J.; Royuela, A.; Sala, A. (2022). Evaluating the use of meteorological predictions in directly pumped irrigational operations using photovoltaic energy. Agricultural Water Management. 266:1-15. https://doi.org/10.1016/j.agwat.2022.107596

Evaluating the use of meteorological predictions in directly pumped irrigational operations using photovoltaic energy.

Carricondo-Antón, JM[1]., Jiménez-Bello, MA[2]., Manzano Juárez, J[1]., Royuela Tomas, A[1]., Sala Piqueras, A[3].

1. Centro Valenciano de Estudios sobre el Riego (CVERT), Universitat Politècnica de València; juacaran@upv.es
2. Instituto de Ingeniería del Agua y del Medio Ambiente (IIAMA), Universitat Politècnica de València
3. Instituto Universitario de Automática e Informática Industrial (AI2), Universitat Politècnica de València

*Corresponding author

Juan M. Carricondo-Antón

Centro Valenciano de Estudios sobre el Riego (CVER)

Universitat Politècnica de València

Camino de Vera s/n, Valencia, Spain

Phone: +34 606 190 339

J.M. Carricondo: juacaran@upv.es

M.A. Jiménez-Bello: mijibar@dihma.upv.es

J. Manzano Juárez: juamanju@agf.upv.es

A. Royuela Tomas: aroyuela@agf.upv.es

A. Sala Piqueras: asala@isa.upv.es

Acknowledgements

A. Sala is grateful to the support of grant PID2020-116585GB-I00 from Agencia Española de Investigación (Spanish government and European Union).

B. This study has been partially supported by the ADAPTAMED project (RTI2018-101483-B-I00), funded by the Ministerio de Ciencia e Innovación of Spain and with EU FEDER funds.

Evaluating the use of meteorological predictions in directly pumped irrigational operations using photovoltaic energy.

Summary

The modernization process in irrigation has generated a higher demand for energy. Due to this problem and the reduction in manufacturing costs of photovoltaic (PV) panels, there has been an increased use of renewable energies, such as PV energy, to power the pumping equipment involved in pressurized irrigation.

On direct pumping when the available solar energy is lower than required by the pumping units, the resulting stoppages can produce unwanted transient effects or even the evacuation of the network.

To avoid these phenomena and reduce the use of conventional energy, this methodology is proposed whereby meteorological predictions, corrected with a Kalman filter, are used to calculate the available PV power and irrigation needs. This methodology is then compared to the traditional programming method that uses historical data and replaces the crop´s evapotranspiration that occurs in a given time period.

The methodology was applied to a real case study, where an irrigation campaign was simulated using a weekly operative time frame. It was found that the use of meteorological predictions allowed PV energy consumption to be improved from 68.7% to 79.3%, while the use of available photovoltaic energy in the case study passed from 11.64% to 13.37%.

Key words: Photovoltaic irrigation, predicting irrigation needs, precision irrigation, energy availability, PVOI.

Nomenclature

DD: Drainage in depth (mm).

ENR_i: Annual irrigation time using conventional energy for each sector (h).

ETc: Crop evapotranspiration (mm).

ETc $_{2019}$: Evapotranspiration of the 2019 (mm).

$ETc_{M_{d-1)}}$: ETc calculated by measurements at meteorological stations (mm).

ETc $_{Predicted}$: Crop evapotranspiration predicted by meteorological predictions (mm).

ETc $_{week\ (-1)}$: Crop evapotranspiration predicted by ETc of the previous week (mm).

$ETc_{K_{week(+1)}}$: ETc prediction corrected with the Kalman filter for the next week (mm).

$ETc_{K_{week(-1)}}$: ETc prediction corrected with the Kalman filter for the previous week (mm).

$ETc_{M_{week(-1)}}$ ETc calculated using weather station measurements from the previous week (mm).

ETo: Reference evapotranspiration (mm).

FC_i: Field capacity of each sector (mm).

fc_{month}: Monthly correction factor of the ETc for citrus.

PV: Photovoltaic

Hm_i: Manometric height required for each sector (m).

I: Irrigation of the previous day (mm).

$Irrad_{2019}$: Irradiance measured in the year 2019 (Wm^{-2})

$Irrad_{10\text{-}years}$: Predicted irradiance using mean data measured from the last 10 years (Wm^{-2}).

$Irrad_{predicted}$: Irradiance predicted by meteorological predictions (Wm^{-2}).

IT: Irrigation time.

$ITacu_i$: Weekly accumulated irrigation time of each sector (h).

$IT_{pv(i)}$: Hours of irrigation using renewable energy during one year by irrigation sector (h).

IT_i: Irrigation hours necessary to meet the needs of the crops for a year by irrigation sector (h).

ITC_i: Irrigation time using conventional energy (h).

$ITmax_{,i}$: Maximum daily irrigation time (h).

IT_{min}: Minimum irrigation time (h).

IT_{std}: Watering time of the previous week (h).

IT_{Pred_week}: Irrigation time predicted by meteorological predictions (h).

Ksat: Hydraulic conductivity in saturated soil (mm).

Kc: Culture coefficient.

IN: Irrigation needs (mm).

P_s: fraction of the FC of soil water

P_e: Effective precipitation (mm).

$P_{min,i}$: Minimum power required by the water pumps for each sector (kW).

$P_{net,d,h}$: Net power available for each day and hour produced by the photovoltaic generator (W).

Pp: is the peak power of the solar panel (W).

$Preal_{d,h}$: Power measured on a certain day at a certain hour (kW).

PVOI: Opportunity Photovoltaic Irrigation.

q : Specific flow per square meter and hour $lh^{-1}m^{-2}$.

Q_i : Flow required for irrigation sector (m^3s^{-1}).

SAT: Saturation humidity (mm).

SI: Solar irradiance (Wm^{-2}).

T: Temperature in (ºC).

$Tcel$: Photovoltaic cell temperature (ºC).

$TONC$: Nominal operating temperature of the photovoltaic cell (in this case 45 ºC).

$W_{crit,\,i}$: Critical soil moisture below which crops are damaged (mm).

$W_{i,d}$: Humidity for each day of the week (mm).

$W_{i,d(-1)}$: Soil moisture of the previous week (mm).

η_{fc}: Inverter efficiency.

η_m: Efficiency of the motor.

η_i: Efficiency of the pumps for each sector.

γ: Specific weight of water (Nm^{-3}).

α_p: Coefficient of variation of Pp with temperature (%/ºC).

Subscripts

i: It refers to the different sectors.

d: Refers to a certain day.

h: Refers to the time of day.

1. Introduction

The global increase in CO_2 emissions and climate change are making the scarcity of available water self-evident; the decreasing rainfall and increasing temperature (Turral et al., 2011), are thought to be reducing water resources between 30% and 50% (Milano et al., 2013). To alleviate the compound effects of climate change, an increasing world population (UN DESA, 2019), and increasing water consumption different plans are being developed around the world to modernize irrigation systems; Spain being a clear example of this (MAPAMA, 2002; MARM, 2010). Modernization has led to an improvement in water efficiency, but with considerable energy cost increases (Espinosa-Tasón et al., 2020), especially in those facilities where the reservoirs supplying the irrigation water do not have sufficient altitude to feed the networks by gravity alone, and so require additional energy inputs. In addition to the increasing energy requirements, the price of this energy has also increased, generating problems of economic viability for many agricultural farms; the situation in Spain being a case in point (García Morillo et al., 2018). Furthermore, in regions such as the Valencian Community, where pressurized irrigation is used on 68% of its irrigable land (mainly on citrus fruit cultivations, making up 53%, and other fruit trees 15%), the use of renewable energies has been incorporated as a central pivot in the proposed plans of the Regional Government (Valencian Strategy on Irrigation (Generalitat Valenciana, 2020)). Photovoltaic energy is more sustainable than conventional energy such as diesel (GIZ, 2016) or other conventional supplies, and with the fall in photovoltaic panel prices, traditional energies have been increasingly replaced by this renewable energy in irrigation pumping.

In the bibliography you can find different articles where energy efficiency has been increased; that is, the power required to supply the irrigation network is reduced by improving the irrigation programming (Díaz et al., 2012; Fernández García et al., 2013; González Perea et al., 2014; Jiménez-Bello et al., 2010; Moreno et al., 2007). Other authors have studied hybrids between renewable and traditional energies, or between different renewable energies, where the feasibility of alternating them in order to satisfy certain energy requirements has been tested (Adamsab et al., 2020; Caldera and Breyer, 2019; El-houari et al., 2020; Elkadeem et al., 2019; Li et al., 2017; Lian et al., 2019; J. W. Powell et al., 2019; Janine W. Powell et al., 2019). Studies have also been carried out that involve the installation of photovoltaic panels that provide the energy to pump and store water in reservoirs at altitudes higher than that of the plantations (Bakelli et al., 2011; Hamidat et al., 2003; Meah et al., 2008). However, this latter option has the problem of the economic and environmental costs involved in the reservoir´s construction, as well as in finding the space necessary, which might entail building the reservoir at some distance from the land requiring the irrigation. For this reason, direct solar powered irrigation systems are being implemented, where solar radiation is used to directly pump with energy accumulation in batteries (Pardo et al., 2019) or without accumulating in batteries (Mérida García et al., 2018; Zavala et al., 2020), provided that the crops are resistant to water stress as indicated by Mérida et al. (2018). Direct irrigation that is carried out only when there is sufficient photovoltaic energy is called Photovoltaic Opportunity Irrigation (PVOI) and presents users with the problem of uncertainty in irrigation time (IT), since it depends on the solar irradiation available (López-Luque et al., 2015).

In irrigation networks that supply many hydrants, each possibly serving several outlets, it is advisable to program the opening and closing of the solenoid valves that control these in advance so that the networks operate properly, avoiding unwanted transient phenomena. PVOI systems that solely depend on photovoltaic energy are exposed to an increase in transient phenomena associated with the inappropriate start-up and stoppage of pumps, or the inopportune opening and closing of outlets, at times when the radiation is not sufficiently intense.

Therefore, this paper presents a proposal where the uncertainty of the PVOI is reduced through the use of weather predictions which allow the estimation of the hours of irradiance and the evapotranspiration reference (ETo) (Li et al., 2018; Santra et al., 2021) within a weekly time frame. Thus, the intention is to know in advance both the available energy times and the required irrigation needs, to suitably schedule irrigation time. In addition, a soil-plant-water model has been incorporated which allows an evaluation of the state of the soil´s moisture so as to establish the irrigation schedule within humidity thresholds that do not harm the crops.

The objective of this study is to evaluate a PVOI programming methodology that uses climate predictions instead of historical data. In this way, it seeks to maximize the use of the irradiance available to the pumping units and to adjust the irrigation doses to the levels that are strictly necessary. This methodology is applied to direct injection systems with multiple hydrants where it is essential to know in advance the system´s operational programming.

2. Materials and methodology

2.1. Case study

The case study focused on the Camí Albalat irrigation network managed by the Massalet Water Use Association. It is located in the municipality of Carlet (Valencia, 39°13'27.45"N, 0°30'8.83"W), in eastern Spain. The Association cultivates adult citrus fruit trees that are irrigated by the waters flowing from the Júcar-Turia Canal. Here, surface irrigation using channels to distribute the water has been replaced by a drip irrigation system. The minimum pressure necessary in each hydrant is 28 m, so pumps powered by a photovoltaic (PV) system have been set up and in addition, for those periods when the PV energy supply is less than that required, they can also be run on conventional electricity. The soil is sandy loam with a hydraulic conductivity (Ksat) of 800 mm day^{-1}, for the calculation of drainage capacity.

The hydraulic network is fed from a 50,000 m^3 reservoir, from which water is directed to two pumping stations that respectively supply the areas of Cami Albalat with 681 ha and the Plaça Massalet with 783 ha.

Irrigation has been organized into operational sectors; each sector consisting of hydrants that irrigate at the same time. The criteria used to create each sector has been empirically determined, trying to ensure that the flows and pressures required at the heads are homogeneous.

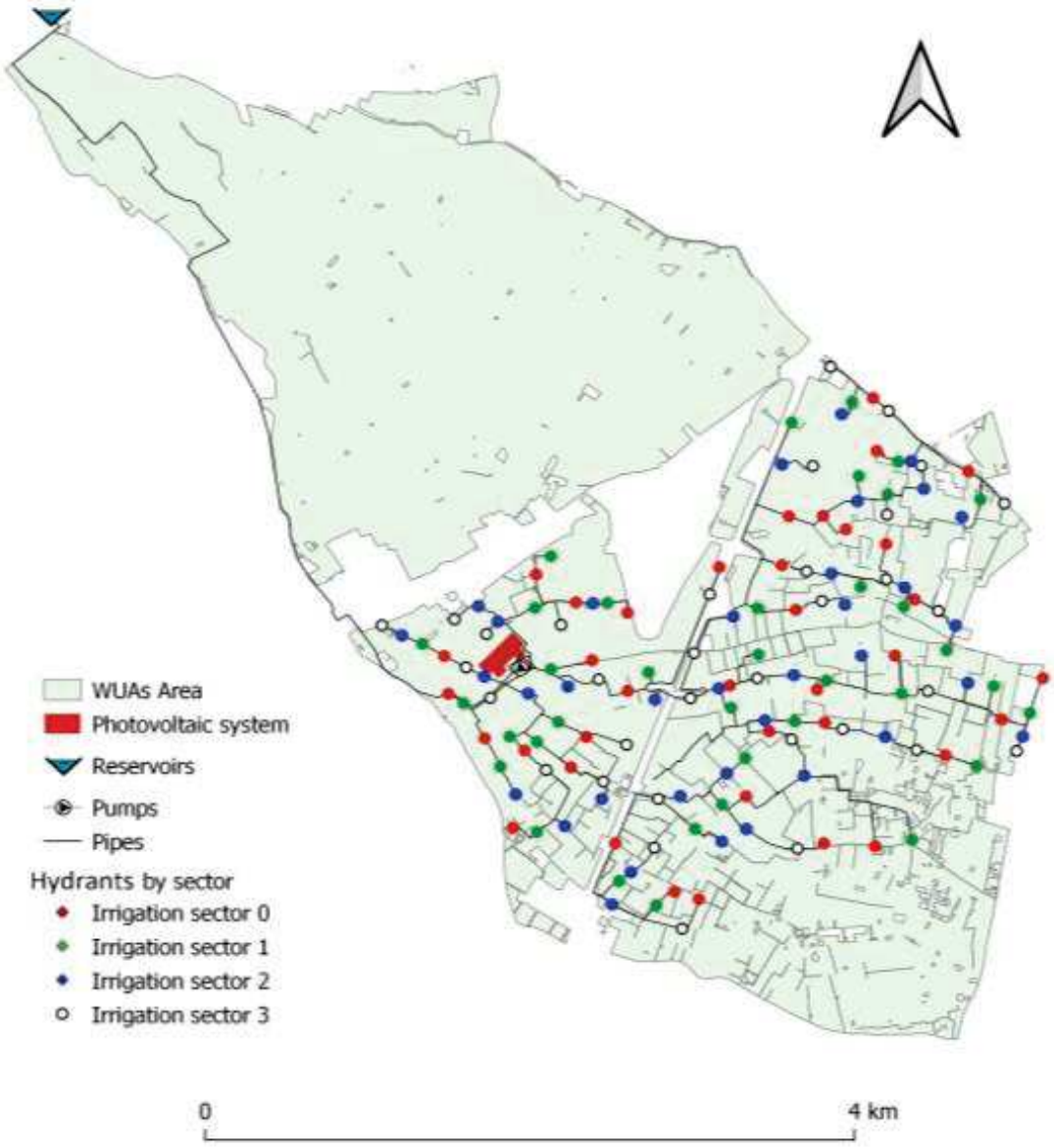

Fig. 1. which describes the layout of the network, shows that the water is collected and conducted via gravity to the pumping station. The hydrants have been grouped according to the irrigation sector to which they belong.

The irrigation network fed by the Cami Albalat pumping station, is at a height of 42.6m and has a total of 147 hydrants with base demand, 198 pipes with a total length of 41528.5m and diameters ranging between DN-90 and DN-710, and a water propulsion system consisting of 3 pumps supplying 4 irrigation sectors. Each hectare has been installed with 4200 emitters of 4 l h^{-1} which is equivalent to 1.68 $lh^{-1}m^{-2}$.

Once the layout of the network, the diameters of the pipes, the demand hydrants and their corresponding flows, together with the characteristic curves of the pumping units were established, the hydraulic network model was constructed using the EPANET hydraulic simulator. The flow in each sector was directly obtained from the pipework downstream of the pumps, and the minimum pumping head (Hm) required for each hydrant, in order to have the minimum service pressure of 28 m, was determined following the process explained by (Díaz et al., 2012; Fernández García et al., 2013; González Perea et al., 2014; Jiménez-Bello et al., 2010).

The pumping equipment is arranged so that the sectors are irrigated by means of the 3 pumps positioned in parallel, generating different minimum power requirements ($Pmin_i$,W) in order to put the pumps into operation. This calculation was attained using the following equation:

$$P_{min_i} = \frac{1}{\eta_i} \cdot \gamma \cdot \mathrm{Q}_i \cdot \mathrm{Hm}_i \quad (1)$$

Where the characteristic equations of head-flow and flow performance of each pumping unit are, with Q measured in $m^3\ h^{-1}$:

$$H_m = 28{,}254 + 0{,}095 \cdot \mathrm{Q} - 0{,}0002 \cdot Q^2$$

$$\eta(\mathrm{Q}) = 0{,}3606 \cdot \mathrm{Q} - 0{,}0004 \cdot Q^2$$

Where η_i is the efficiency of the pumps for each sector, γ is the specific weight of the water (Nm^{-3}), Q_i is the flow required for each irrigation sector (m^3s^{-1}) and Hm_i is the head required by each sector (m).

For the pumps to operate 100% under PV power it is necessary that the energy supplied by the PV system is greater than the minimum energy required by the pumping system. For each sector, the heads (m), flow rates (m^3s^{-1}) and minimum power requirements (kW) were calculated.

The PV system consists of 912 panels, each made up of 72 PV 6 inch cells of polycrystalline material which together produce 325 W. The panels occupy an area of 1773 m^2 with the capacity to generate 296.4 kW. In addition, the PV system is formed by 3 variable frequency inverters.

The PV installation designed by the technicians of the water-use association is arranged in such a way that the hours and energy produced by the PV panels are greater than the hours and energy required by the pumps for most of the time. The ratio between the rated energy capacity of the PV generator and the power needs of the sector with the highest $Pmin_i$ is 2.23.

Despite this design ratio, there may be weather conditions where the PV system does not receive sufficient irradiance. When the irrigation needs cannot be supplied by PV energy, the pumping station is supplied by conventional energy in order to complete the irrigation hours. The annual IT using conventional energy for each sector (EIN_i,h) was calculated using the following equation:

$$EIN_i = \sum_1^i \left(IT_i - IT_{pv(i)}\right) \quad (2)$$

Where IT_i are the hours of irrigation necessary to provide for the needs of the crops during a year as per irrigation sector, and ITpv(i) are the hours of irrigation provided by renewable energy during a year per irrigation sector.

2.2. Description of the methodology

There was a clear intention to reduce the consumption of conventional electrical energy and adjust the consumption of water to that which was strictly necessary by establishing in advance the operation of the outlets and pumping equipment so as to ensure the correct functioning of the PVOI system.

For these purposes, weather forecasts were used to estimate the irrigation needs and hourly irradiance.

The estimated irrigation needs, temperature and irradiance were initially calculated using the standard methodology described in section 2.3. Subsequently, the calculations of the predicted irrigation needs, temperature and irradiance were determined using the methodology based on weather predictions corrected with the Kalman Filter, to account for micro-scale biases between the gross-scale predictions from meteorological data and the actual sensor readings at the fields, as described in section 2.3.2.

Having estimated the irradiance and temperature, the energy that would be generated by the PV system using the second method was determined.

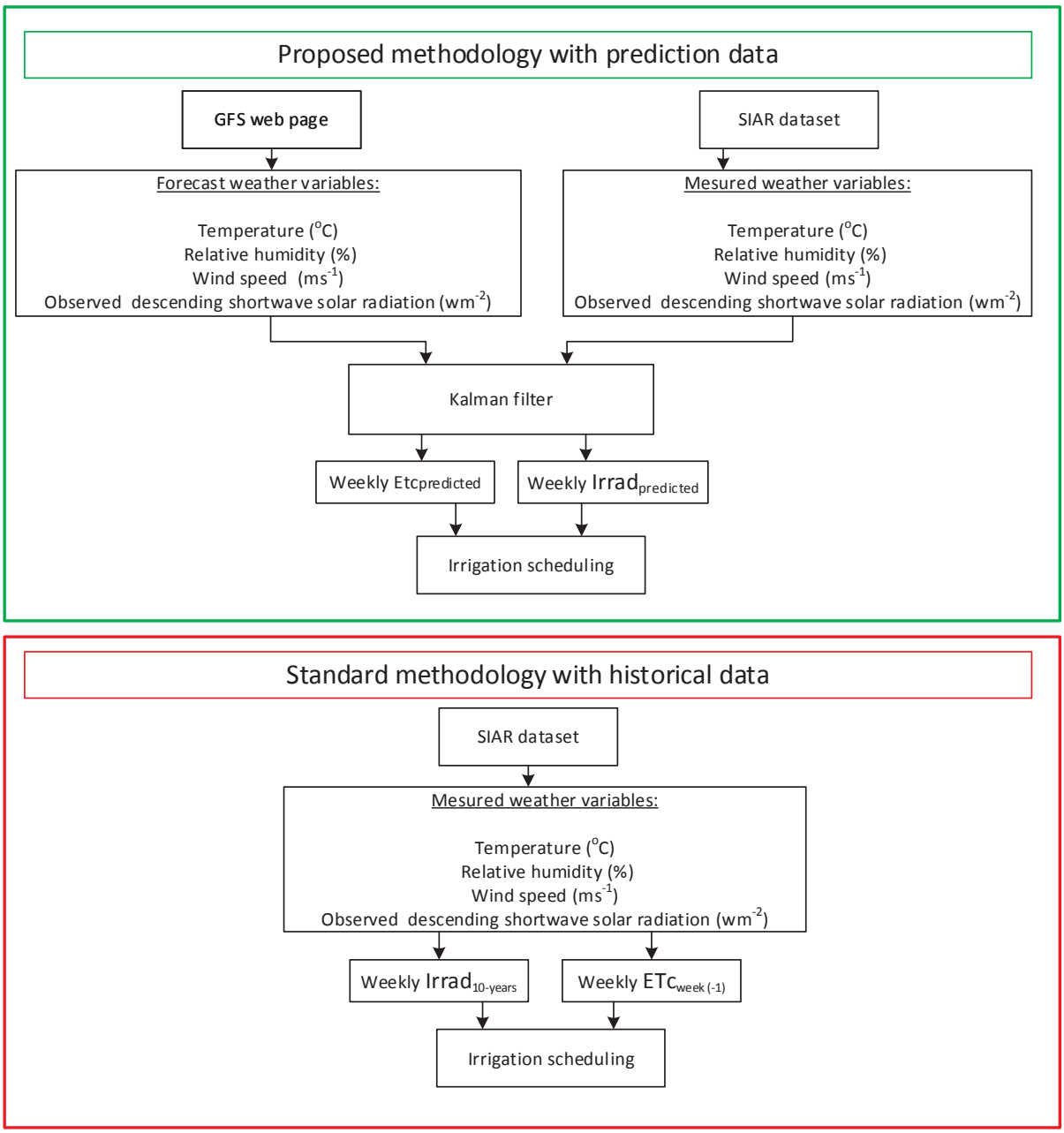

Fig. 2. Workflow chart of the proposed methodology to evaluate the use of weather forecast data and historical data for irrigation scheduling.

Finally, once the capacity of energy generation within a week, the cumulative irrigation time needed for that week, and the energy required by the water pumps were known, the programming of the irrigation sectors was determined in such a way that Eq. 2 was minimized and the moisture in the soil did not produce crop stress, while avoiding drainage. To do this, the representative Field Capacity of each sector (FCi) was obtained and the soil moisture was calculated for each day of the week and sector ($W_{t,d}$). In addition, a simulation with 2019 data is carried out to validate the methodologies.

This methodology was applied to sectored irrigation, as described in Section 2.1. Sectors can operate with a constant setting pressure for all of them, determined by the most

unfavourable sector, or a variable setting pressure is established for each sector. To simplify the number of hypothesis, it was assumed that it was possible to establish a variable setting pressure for each sector.

Before scheduling the irrigation, the FCi was determined. This term can also be replaced by the target moisture to be maintained in the soil (Martínez-Gimeno et al., 2018), or the humidity for each day of the week Wi,d. This humidity must not be less than the critical value that may cause excessive stress to the crop (Wi,crit) as described in the section. 2.4. In the same way, a minimum irrigation time period (ITmin) was determined during which the pumps must be activated to avoid irrigations lasting only short durations, ensuring in this way that where the system does manage to reach the steady state.

The determination of the irrigation schedule, that is, when each sector is irrigated each week, was carried out as follows:

1. The weekly irrigation time was calculated for each of the sectors. In this case it was the same irrigation time for each of the sectors (IT_{std} o $ITPred_{\_week}$) (see Section 2.3.1).
2. For each sector, each day the accumulated irrigation time $ITacu_i$ was calculated, which at the end of the week had to be equal to IT_{std} o $ITPred_{\_week}$. This irrigation time was carried out either with PV energy or with conventional energy.
3. The net hourly power $\mathrm{Pnet}_{\mathrm{D,H}}$ was determined for each of the hours and days of the week (see Section 2.5).
4. The irrigation sectors were ordered according to the $P_{min,i}$ from highest to lowest.
5. Peak hours Pnet were assigned to sectors when $P_{net} \geq Pmin_i$.
6. Starting from the sector with the greatest $Pmin_i$ a loop was formed running down the hours of each day of the week.
7. The maximum daily irrigation time $ITmax_{,i}$ was determined for each sector, as long as $P_{net} \geq Pmin_i$, until it reached FCi; $ITmax_{,i}=\{IT_{std}, ITPred_{\_week}\}$. If $ITmax_{,i}$ was positive, or if $W_{i,d} < W_{crit,i}$, irrigation was carried out.
8. For the sectors where irrigation was carried out, whether $P_{net,i} < Pmin_i$ was checked. In the cases that it was affirmative, that hour was assigned until $ITacu_i = ITmax_{,I}$. The consumed hours were ruled out for the following sectors. In the cases where $P_{net,i} < Pmin_i$ and $W_{i,D} < W_{crit,i}$ conventional energy was used.
9. Sector i did not irrigate again until $ITmax_{,i}$ was positive and higher than IT_{min}.
10. The loop repeated itself for each day of the week and for each sector.

At the end of the weekly programming $ITacu_i \leq ITmax_i$. It should be noted that $ITacu_i$ may be less than $ITmax_i$ when the soil is in FCi or when $ITmax_{,i} < IT_{min}$.

To evaluate the proposed methodology, $Pmin_i$ was compared with the actual net hourly power that occurred during that hour and that day ($Preal_{d,h}$).

If $Preal_{d,h} > Pnet_{d,h}$ the system was assumed to be powered by PV and counted as IT_{pv}. In cases where $Preal_{d,h} < Pnet_{d,h}$ it was assumed that the system was working with conventional energy and the irrigation hours were counted as ITC_i.

This process was repeated for the entire 2019 irrigation campaign with a weekly frequency, taking Monday as the day of reference.

This paper conducted a comparative analysis of the irrigation results obtained under different scenarios, dependant on the irradiance and ETo computation methods chosen, in order to find out which methods were better to maximize the use of PV energy and reduce water consumption.

With regard to the computation of irradiance, a first and third scenarios based the ensuing week´s irradiance on predictions arising from meteorological data ($Irrad_{predicted}$) instead (SCE1 and SCE3), whereas a second scenario considered irradiance in the forthcoming week to be equal to that week´s average radiation over the last 10 years ($Irrad_{10\text{-}years}$) (SCE2 and SCE4). In relation to ETo estimations, two options were also considered: one considered ETo to be equal to the value that was attained the previous week by this indicator (SCE3 and SCE4), and the other used a predicted ETo value (SCE1 and SCE2). In summary, there are four possible scenarios if all the options are considered, as depicted in Figure 3. See Section 2.3 for more details.

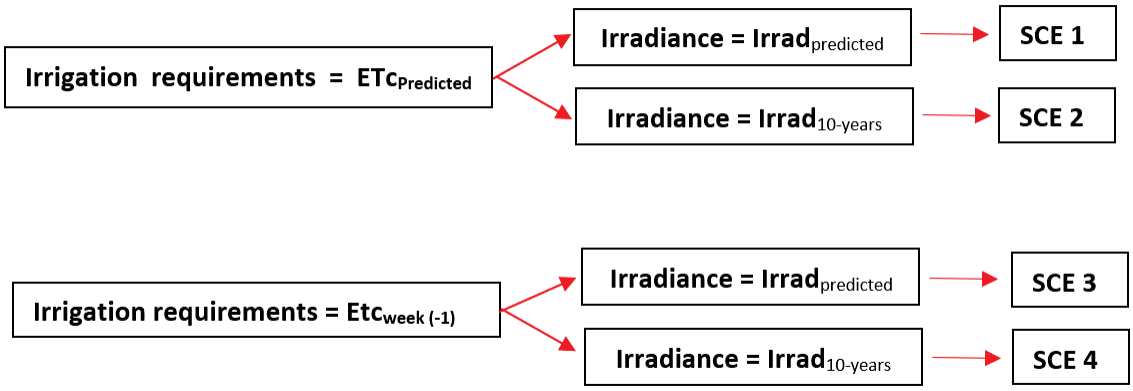

Fig. 3. 4 Scenarios: 2 scenarios by ETo calculation methodology; by means of meteorological predictions, SCE1 and SCE2, and by ETo of the previous week, SCE3 and SCE4 and 2 scenarios by type of predicted irradiance type, SCE1 and SCE3 by means of meteorological predictions and by means of average data of the last 10 years, SCE2 and SC4.

Once the SCE1, SEC2, SCE3 and SEC4 scenarios were defined, a simulation of the evolution of soil moisture is carried out, using an agrohydrological model which allows determining the irrigation dose (volume of water supplied) and the drainage for each scenario. In addition, the photovoltaic and conventional energy used for each scenario is studied through irrigation scheduling. The results obtained are evaluated using the data observed in meteorological stations in 2019 year (see figure 4).

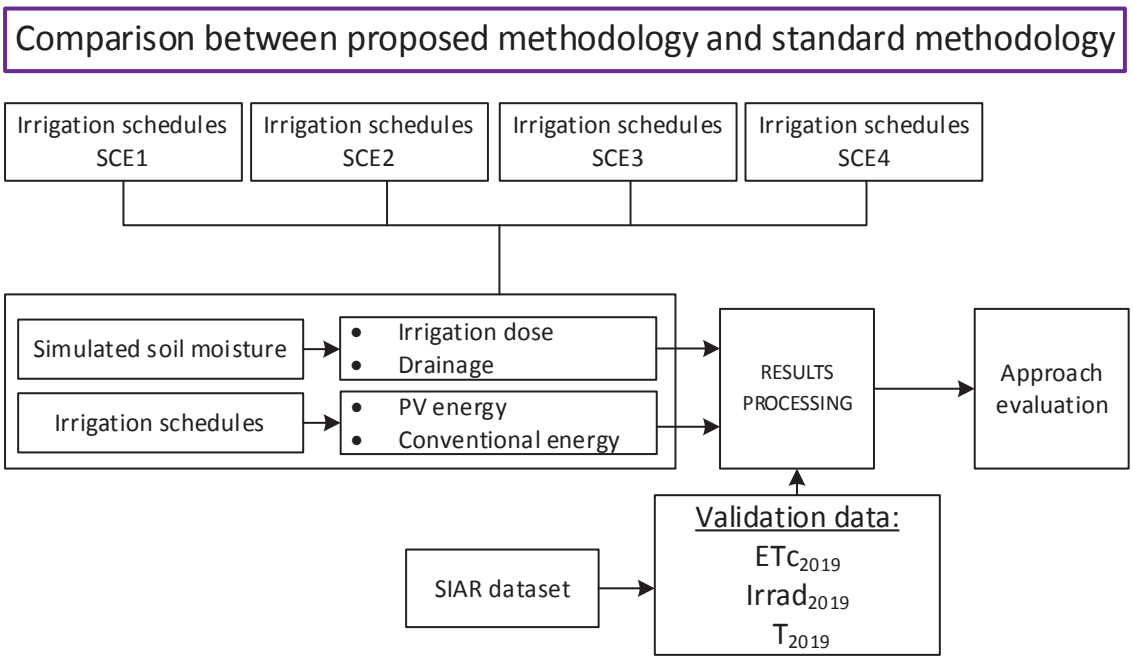

Fig. 4. Comparison between proposed methodology and standard methodology

2.3. Calculation of Irrigation Needs (IN)

To determine the irrigation needs, Penman Monteith's methodology (Allen et al., 1998) was used to calculate the ETo. Once the ETo was known the evapotranspiration needs of the crop (ETc) could be determined, using for this purpose crop coefficients based on the percentages of vegetation cover corrected by a monthly correction factor fc_{month} (Castel, 2000) . It was assumed that all the plots had a vegetation cover greater than 70%. Once the ETc was calculated, this was offset by the effective precipitation (Pe). Hence, irrigation needs are the difference between the crops' needs due to evapotranspiration and the precipitation value.

$$ETc = ETo \cdot Kc \cdot fc_{month} \quad (3)$$

$$IN = ETc - P_e$$

The ETo was calculated using two methods:

a) The first method calculated the ETo using the weather predictions for the forthcoming week (i.e. 7 days) in relation to the following respective variables: the average temperature (°C), the relative humidity (%), the wind speed at the height of 2 meters (ms^{-1}), and the observed descending shortwave solar radiation (Wm^{-2}), which is equivalent to the irradiance.

b) The second method calculated the irrigation needs for the following week using the ETo of the previous week, based on the meteorological data obtained from the agroclimatic weather stations belonging to the Agroclimatic Information System for Irrigation (SIAR, in Spanish initials) (http://eportal.mapa.gob.es/websiar/Inicio.aspx). In the case study considered here, this corresponded to the Carlet agroclimatic station located 3786m from the Cami Albalat irrigation pumping station.

2.3.1. Determination of the irradiance and irrigation time using traditional methods

In this section, the irradiance of the week is calculated with the average radiation observed during the same week of the last 10 years, which was measured in the horizontal plane using a Pyranometer model CMP3 (Kipp & Zonen BV Delft, The Netherlands) and save the measured data in the SIAR network, to program the irrigation of the next week.

The standard IT (IT_{std}) is traditionally determined by accepting the ETo of the previous week (Li et al., 2018). However, in the actual study so that both methodologies could be comparable it was decided to compensate the error in the ETo of the previous week, present in the irrigation time taking place the following week, by means of the following equation:

$$IT_{std} = (ETc_{week(+1)} - (ETc_{week(-1)} - ETc_{M_{week(-1)}}) - P_{e_{week(-1)}}) \cdot q^{-1} \quad (4)$$

Where $\mathrm{ETc}_{\mathrm{week}(+1)}$ is the ETc prediction for the following week, $\mathrm{ETc}_{\mathrm{week}(-1)}$ is the ETc prediction for the previous week, $\mathrm{ETc}_{\mathrm{M}_{\mathrm{week}(-1)}}$ is the ETc calculated using weather station measurements from the previous week, $\mathrm{P}_{\mathrm{e}_{\mathrm{week}(-1)}}$ is the effective precipitation during the previous week and q are the $lh^{-1}m^{-2}$.

If IT_{std} was less than 0 or if IT_{std} was less than IT_{min}, no irrigation occurred.

2.3.2. Predictions of meteorological data and irrigation time using the Kalman filter.

The IN of the crops was obtained using the weather forecasts (Carricondo-Anton et al., 2019; Li et al., 2018; Lorite et al., 2015) emitted by the meteorological service, Global Forecast System (GFS) of the National Centers for Environmental Prediction (NCEP), belonging to the USA government. This service provides real-time weather forecasts four times a day, which allowed future ETo to be predicted, and thus determine the irrigation scheduling. This service is offered freely and permits the automatic daily download of predictions (https://www.noaa.gov). However, the problem with the predictions is the uncertainty of the estimates (Dorado and Ruíz, 2018; Evensen, 2003), which do not adapt themselves to the particular casuistry found in each farm (microclimate, orientation, etc.). The horizontal resolution of the grid used in the meteorological simulations is of 28 km and this makes, on the one hand, the accuracy of the simulations decrease and, on the other hand, it means that local phenomena that affect (broadly speaking) areas smaller than 50 km in diameter cannot be simulated. In order to reduce the uncertainty between the predictive model and the measurements taken in weather stations the study employed a Kalman Filter (Kalman, 1960) which is used in meteorology at the surface level (Han et al., 2014; Hunt et al., 2007) and to determine the ETo (Carricondo-Anton et al., 2019; Li et al., 2018).

If we review the basic theory, the Kalman Filter makes predictions with a model $x_k = Ax_{k-1} + Bu_k + w_{k-1}$ from which the measures $z_k = H_k x_k + r_k$ are obtained, *x* being the state (variables to be estimated), *u* the value of possible inputs known to the model, and w_k and r_k are "process" and "measurement" noise respectively, of a known variance-covariance matrix, which will be denoted by Q and R. Our model tried to explain the difference between the observed weather measurement z_k and the weather prediction x_k by means of a linear transformation to the prediction (of slope θ_1 and offset θ_2, that is $z = p_k\theta_1 + \theta_2 = [p\ 1]x$) whose coefficients can vary over time and were therefore incorporated into the vector x of variables to be estimated and their value was adjusted using Kalman's equations as and when "p" predictions and real measures were contrasted; the estimated values of these coefficients were the components of the estimated $\hat{x}_k$, and the Bu component did not need to be part of the model since there were no measurable exogenous *u* components that were additional to the meteorological measurements *z* , leaving $\hat{x}_k^- = A\hat{x}_{k-1}$. The matrix A was the discrete integrator model (the identity), because we assumed that θ_1 and θ_2 were constant (strictly speaking, they follow a random movement –Brownian motion–excited by w_k). The variance Q parameterized the uncertainty in the aforementioned random motion, and allowed the rate of variation to be encoded "a priori" in the times of the adjustable parameters. The matrix H_k was formed with $[p_k\ 1]$ as indicated above. The equations of this filter have two stages (Albertos and Sala, 2004; Dorado and Ruíz, 2018). When a measure was available, the "corrector" step was undertaken and given by:

$$K_k = P_k^- H_k{}^T (H_k P_k^- H_k{}^T + R)^{-1} \tag{5}$$

$$\hat{x}_k = \hat{x}_k^- + K_k(z_k - H_k\hat{x}_k^-)$$

$$P_k = (I - K_t H_k)P_k^-$$

Where P_k^- is the state variance matrix, or the estimation error, H_k is the measurement matrix, K_k is the Kalman gain, z_k is the actual observation at instant k, x is the estimated initial state, and R is the variance matrix of the measurement noise.

Once the corrected vector was obtained for the measures from the data and the past model, the future prediction was determined by adjusting the model of the following days, using the simulation equations (Albertos and Sala, 2004; Dorado and Ruíz, 2018), usually called the "predictor" stage in the literature:

$$\hat{x}_k^- = A\hat{x}_{k-1} \tag{6}$$

$$P_k^- = AP_{k-1}A^T + Q$$

Where P_k^- is the state variance matrix or estimation error, $\hat{x}_{k-1}$ is the estimated state in the previous iteration (or the initial conditions in the first iteration). If one wanted to simulate

several steps in the future without intermediate observations, this is established in the predictor (6) $P_k = P_k^-$, without carrying out the corrector equations (5).

Entering the data into the four Kalman filters, the two parameters of the correction were obtained (recursively) for each of the variables of temperature, humidity, wind at 2m and irradiance (van Mourik et al., 2019). The z_k measures in the filter equations were the observed values of each of these variables at the instant at which the prediction p_k made reference (evidently, the measurement was taken after the knowledge of the prediction, updating the filter in due course once the measurement was available).

The one-week rain prediction was not used because the error that was produced in estimating the amount was unacceptable and without any type of correlation.

With these adjustments we obtained the correction of the previous parameters, the latter also being used to predict the irradiance that would occur the week after. By means of the 4 parameters, the ETo was calculated using the Penman Monteith methodology described in (Allen et al., 1998). Once the IN was known, the predicted irrigation time $ITPred_{\_week}$ was determined, and corrected each week with the error of the previous week, using the following equation:

$$IT_{Pred_{week}} = (ETc_{K_{week(+1)}} - (ETc_{K_{week(-1)}} - ETc_{M_{week(-1)}}) - P_{e_{week(-1)}}) \cdot q^{-1} \quad (7)$$

Where $ETc_{K_{week(+1)}}$ is the ETc prediction for the following week, $ETc_{K_{week(-1)}}$ is the ETc prediction for the previous week, $ETc_{M_{week(-1)}}$ is the ETc calculated using weather station measurements from the previous week, $P_{e_{week(-1)}}$ is the effective precipitation from the previous week and q are the $lh^{-1}m^{-2}$ that can be provided as irrigation flow.

If IT_{std} was less than 0, or if IT_{std} was less than IT_{min}, no irrigation occurred.

2.4. Moisture in the soil

In this study it was important to know the moisture in the soil since the investigation expected to improve water use as well as energy efficiency. By having PV panels, the consumption of electricity based on conventional energies can be reduced. However, irrigation time must also be adjusted to take into account soil moisture, and so avoid making these times excessive up to the point of losing water through drainage.

The determination of soil moisture for each sector $(W_{i,d})$ was established daily, using the equation:

$$W_{i,d} = W_{i,d(-1)} - ETc_M + I + P_e - DD \quad (8)$$

Where $W_{i,d(-1)}$ is the soil moisture from the previous day (mm), ETc_M is the ETc calculated by means of measures taken at weather stations (mm), I is the irrigation (mm), P_e is the effective precipitation (mm) and DD is the deep drainage (mm). This model was simplified by not taking into account surface runoff, as it was a localized irrigation. It was assumed that ETc_M and P_e were the same for each sector.

The calculation of DD was performed when the soil moisture was between Saturation (SAT) and Field Capacity (FC), the drainage being calculated using the following equation (Raes, 1982; Raes et al., 2006, 1988).

$$DD = 0.0866 \cdot Ksat^{0.35} \cdot (SAT - FC) \quad (9)$$

Following the guidelines of (Allen et al., 1998), the fraction of the FC of the soil water (p_s ,%) was used so that citrus crops with a coverage greater than 70% did not suffer stress. This fraction limits the minimum amount of water (mm) that the soil should contain so that citrus crops do not suffer stress. This was done according to the equation:

$$W_{crit,i} = 0.5 + 0.04 * (5 - p_s \cdot ETc_{(mm \cdot dia^{-1})}) \quad (10)$$

2.5. Photovoltaic system

The efficiency of the PV cells that make up a PV panel is affected by the temperature they can reach when subjected to irradiance. To calculate the temperature of the cell (Tcel, ^{o}C) the following formula was employed (Markvart and Castaner, 2003).

$$Tcel = T + \frac{(TONC-20) \cdot SI}{800} \quad (11)$$

Where T is Temperature in (^{o}C), *TONC* is the nominal operating temperature of the PV cell (in this case 45 ^{o}C) and *SI* is solar irradiance (Wm^{-2}).

The calculation of the available net hourly PV power for each day of the week was determined by the equation:

$$P_{d,h} = P_p \cdot \frac{SI}{1000} \cdot \left(1 + \frac{\alpha_p}{100} \cdot (Tcel - 25)\right) \quad (12)$$

Where *Pp* is the peak power of the PV plate, *SI* is the mean hourly irradiance (Wm^{-2}), α_p is the coefficient of variation of Pp with temperature (%/^{o}C) and *Tcel* is the temperature of the PV cell. Finally, it should be taken into account that the net available power to the pumps for

each hour and day of the week ($Pnet_{d,h}$) is affected by the efficiencies of the inverter and the motor of the equipment.

$$P_{net,d,h} = P_{d,h_i} \cdot \eta_{fc} \cdot \eta_m \quad (13)$$

Where η_{fc} is the estimated efficiency of the inverter which is 0.9, and η_m is the estimated efficiency of the motor which is 0.8.

During those weeks where the irrigation hours and energy required were greater than the hours and energy supplied by the PV installation, irrigation occurred by means of conventional electricity (Mérida García et al., 2019).

3. Results and discussion

The results from the different scenarios are described in two sections. The first section analyses the favourability of the predictions with regards to water needs, irradiance, temperature and Pnet, while the second section analyses the network´s irrigation programming using the meteorological predictions. The purpose is to assess whether the use of predictions, and the errors committed with them, leads to an enhancement of the irrigation programming and, in turn, to an improvement in the use of water and PV energy, while reducing conventional energy consumption.

3.1. Evaluation of predictions

3.1.1. Assessment of irrigation needs

Firstly, to determine the flow rates and $Pmin_i$ of each of the four sectors making up the network, each with different Hm_i and Q_i, a hydraulic analysis was performed. The results are shown in Table 1.

Table 1.

Data by sector of Hm, Q and Pmin requirements for the three pumps operating in parallel.

	Hm (m)	Q (m^3/h) 3 Pumps	Pmin (KW)
Irrigation sector 0	25,0	1491,0	128,6
Irrigation sector 1	25,6	1345,4	115,6
Irrigation sector 2	24,4	1314,0	107,6
Irrigation sector 3	28,0	1413,7	132,8

The irrigation needs have been obtained by means of the predictions comparing $ETc_{Predicted}$ and $ETc_{week\ (-1)}$ against ETc_{2019} (actual ETc in 2019), resulting in 720.9 mm $year^{-1}$ (SCE 1, SCE 2) and 728.7 mm $year^{-1}$ (SCE 3, SCE 4) and 715.5 mm $year^{-1}$ respectively. Figure 5 shows the weekly irrigation time for the $ETc_{Predicted}$ (SCE1, SCE2), the $ETc_{week\ (-1)}$ (SCE3, SCE4) and ETc_{2019}.

Having determined the volume of water required, the irrigation time were calculated, firstly, by means of the weather predictions, resulting in 429.1 h sector^{-1}year^{-1} of irrigation, and secondly, using the ETc of the previous week (methodology traditionally used) obtaining 433.8h sector^{-1}year^{-1} of irrigation. This represents a saving in IT and water volume of 1.1% per year.

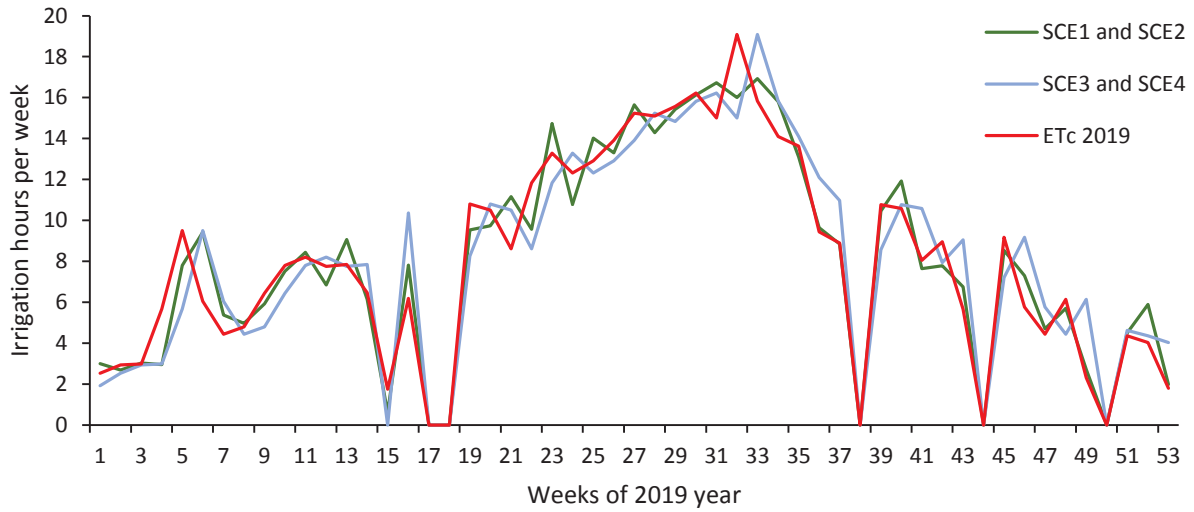

Fig. 5. Irrigation time with weekly ETc predicted by meteorological predictions (mm) (green), weekly ETc predicted by ETo of the previous week (mm) (blue) and weekly ETc calculated by meteorological measurements (mm) (red).

The ETc was determined on a weekly basis each Monday for every week in 2019, both for the ETc $_{Predicted}$ (SCE1, SCE2) and the ETc $_{week\ (-1)}$ (SCE3, SCE4). As can be seen in Table 2, we analysed the average weekly error of the ETc $_{Predicted}$ and ETc $_{week\ (-1)}$ for the period of maximum IN (from April 1st to September 30th), for the periods of minimum IN (from January 1st to March 31st and from October 1st to December 31st), and the entire year 2019, as well as the maximum and minimum relative errors and the percentage of standard deviation that occurred. The relative error for uncompensated ETc$_{Predicted}$ was 9.9% while for the uncompensated ETc $_{week\ (-1)}$ (historical data) it increased to 24.8%. Once ETc $_{Predicted}$, and ETc $_{week\ (-1)}$ had been compensated, as indicated in sections 2.3.1. and 2.3.2., the relative error for compensated ETc $_{Predicted}$ analysed amounted to 12.4%, while for the historical data the compensated ETc $_{week\ (-1)}$ increased to 24.1%. Table 2 shows the relative errors for ETc $_{Predicted}$ and ETc $_{week\ (-1)}$. The ETc compensated with the previous week´s error was greater than the error of the ETc because compensating from the previous week can generate a greater difference relative to the ETc of the week to be predicted. However, the convenience of using the compensated ETc is due to the fact that throughout the year the same amount of mm is irrigated as the ETc of that year.

Table 2

Analysis of relative ETc prediction errors, both compensated and uncompensated for the error of the previous week (%) for the periods of maximum IN, minimum IN and for the rest of the year.

	Etc		Compensated Etc	
	$ETc_{Predicted}$	$ETc_{week\ (-1)}$	$ETc_{Predicted}$	$ETc_{week\ (-1)}$
	SCE1 y SCE2	SCE3 y SCE4	SCE1 y SCE2	SCE3 y SCE4
Relative square error in time of maximum IN (%)	6,3	15,2	10,5	16,5
Relative square error in time of minimum in (%)	13,3	34,1	14,2	31,4
Annual Square error (%)	9,9	24,8	12,4	24,1
Maximum error (%)	43,7	165,1	65,2	165,1
Minimum error (%)	0,4	1,0	0,0	0,0
Typical deviation (%)	10,5	29,7	14,2	31,8

From here it can be determined that the relative errors are lower for $ETc_{Predicted}$ than for $ETc_{week\ (-1)}$, so it is advisable to use the former to determine the IN.

3.1.2. Evaluation of sectors according to soil moisture content

This section presents the soil moisture results achieved for the 4 scenarios SCE1, SCE2, SCE3 and SCE4. In the 4 graphs below the sectors requiring minimum and maximum power for the pumps to operate are represented. As table 1 indicates the sector that required the most energy was sector 3 and the sector that required the least energy was sector 2.

The effective precipitation and minimum soil moisture required so that plants would not suffer stress have also been represented. In none of the 4 scenarios did the plants suffer stress because there was a lower limit of humidity beyond which irrigation always took place, fixed at 25% of the FC_i which in this case was 82.5 mm. If this percentage is decreased, the number of hours irrigated by PV energy is increased, but the crop approaches the threshold of water stress.

It can be observed that the humidity in the sector of maximum power requirements for pumping did not usually reach the minimum humidity established, this is because it was the sector that first took advantage of the hours of available energy. In contrast, the sector with the minimum power requirement for pumping did reach the minimum humidity established because it was the last sector to be irrigated throughout the week and therefore this sector was the one that required more electrical energy, due to the low humidity of the soil.

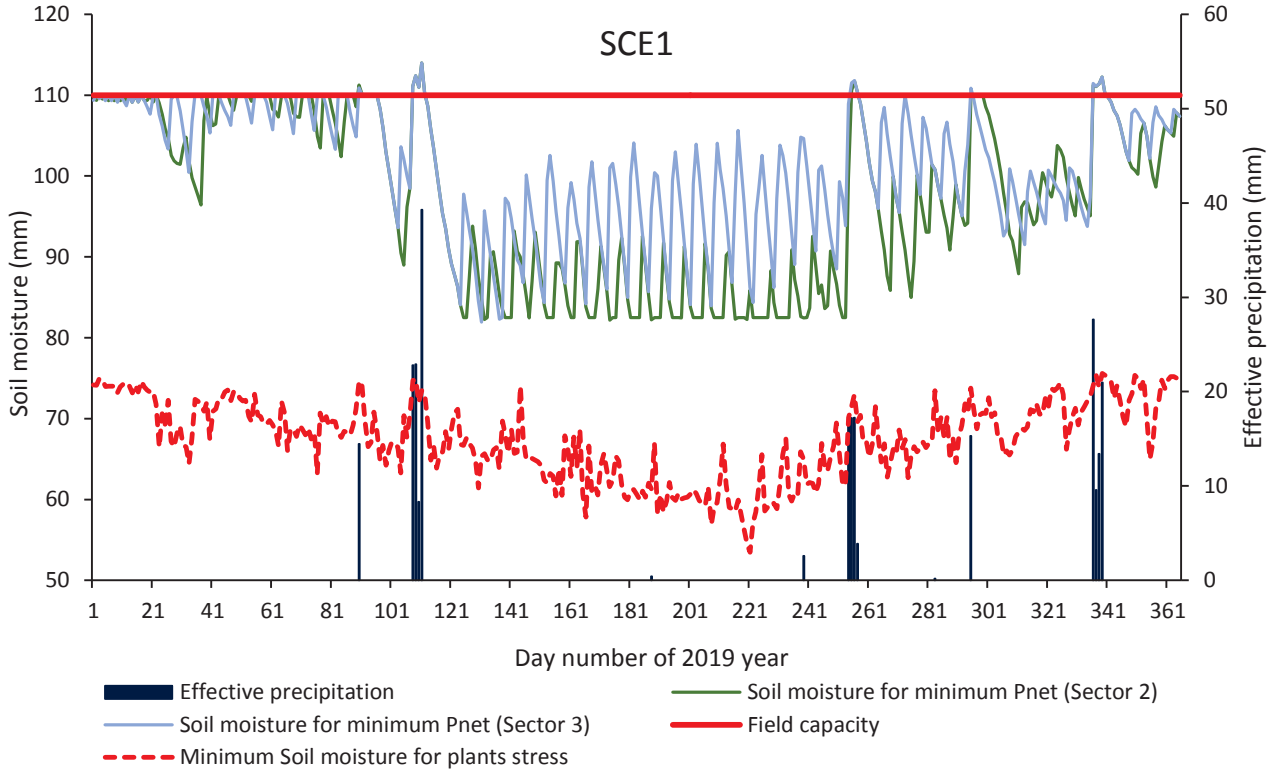

Fig. 6. Field capacity, soil moisture by predicted ETc and predicted irradiance with meteorological predictions and minimum soil moisture for stress in citrus.

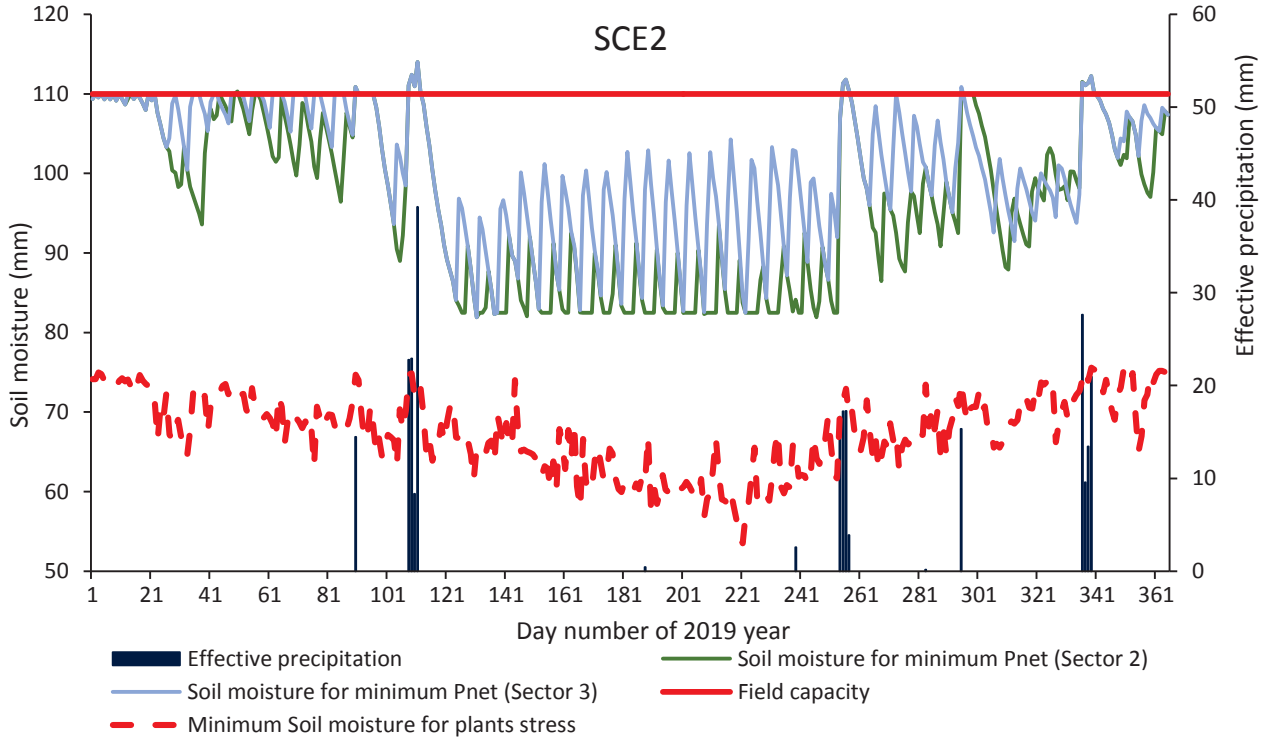

Fig. 7. Field capacity, soil moisture by ETc predicted with meteorological predictions, mean irradiance of 10 years and minimum soil moisture for stress in citrus

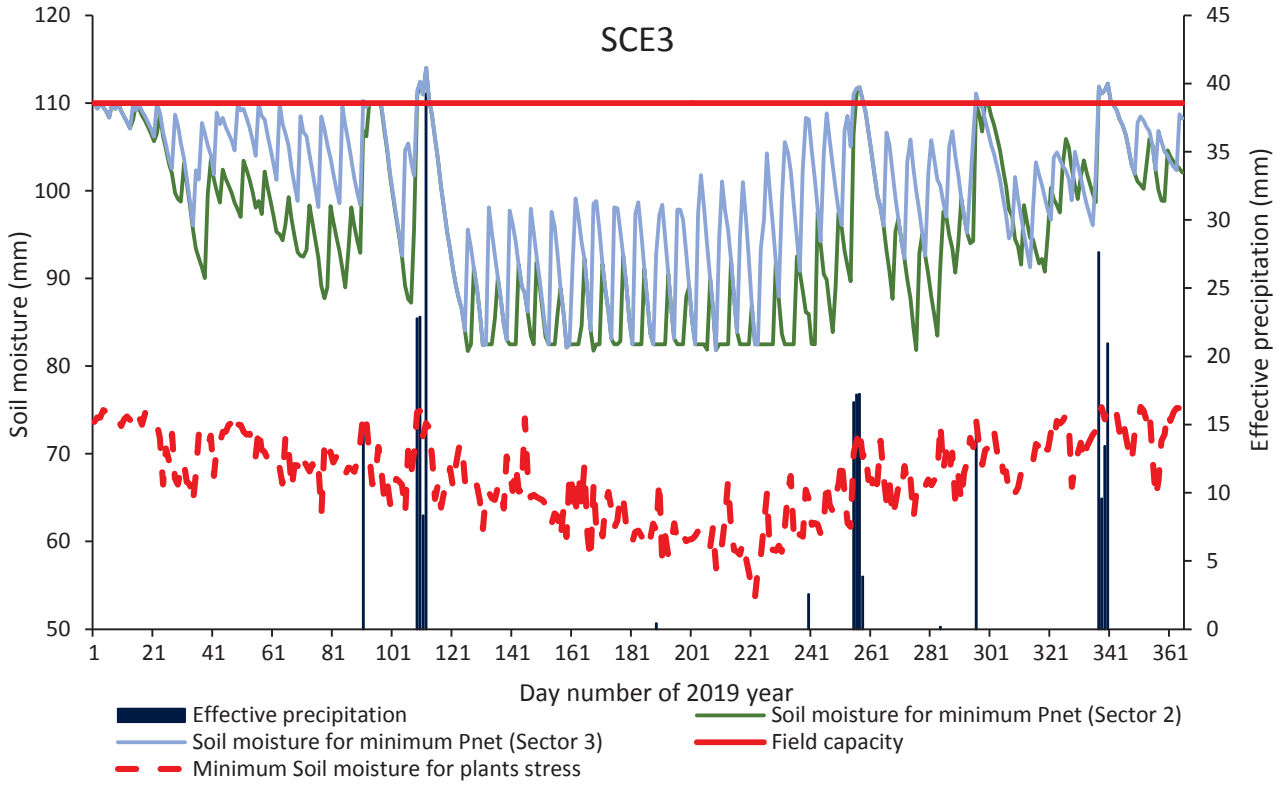

Fig. 8. Field capacity, soil moisture by ETc from the previous week and irradiance predicted with meteorological predictions and minimum soil moisture for stress in citrus.

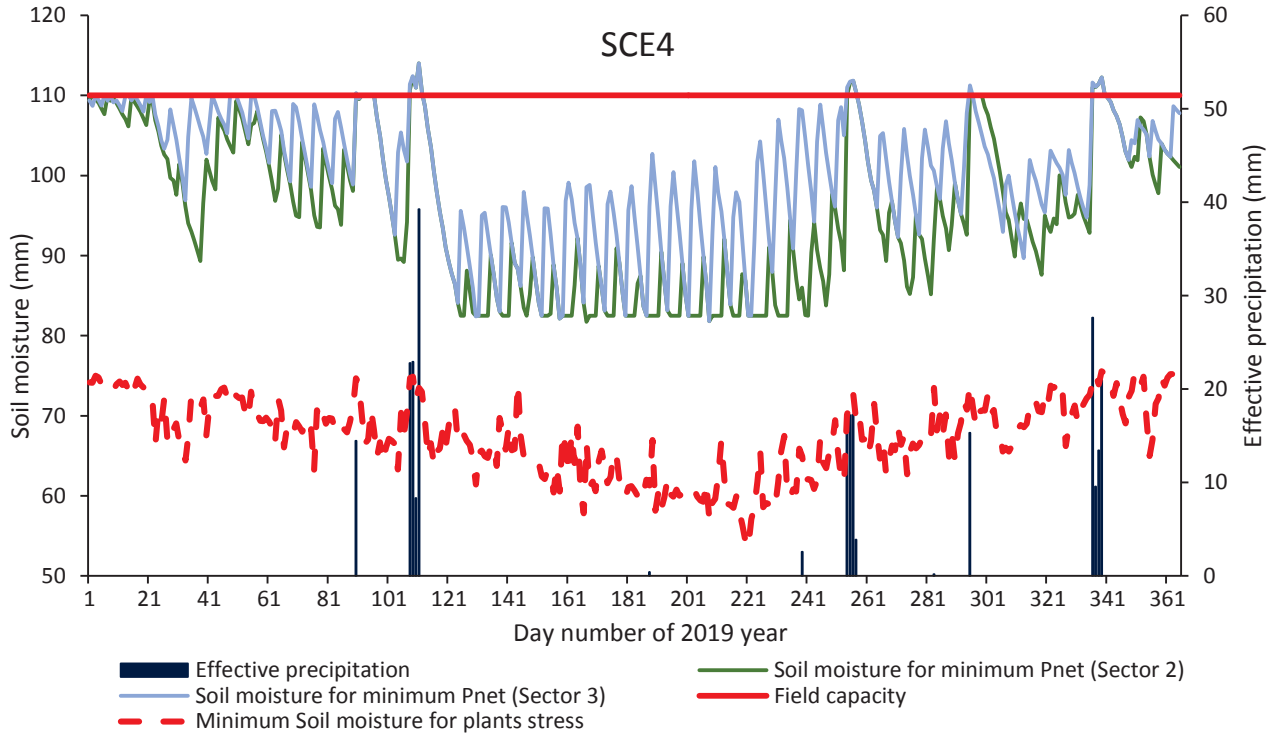

Fig. 9. Field capacity, soil moisture by ETc from the previous week, mean irradiance of 10 years and minimum soil moisture for stress in citrus.

3.1.3. Evaluation of irradiance, temperature and net power for photovoltaic pumping

The highest monthly irradiance coincided with the highest irrigation needs (Mérida García et al., 2018; Zavala et al., 2020) as can be seen in Figure 10. Upon calculating the average monthly irradiance in $kWhm^{-2}dia^{-1}$ we observe that when comparing the $Irrad_{predicted}$ and the irradiance measured in 2019 ($Irrad_{2019}$) there was an average relative error every month of 3.68%, and when comparing the $Irrad_{10\text{-}years}$ with respect to that measured in 2019 there was an average relative error every month of 6.7%. This justifies the relevance of our proposal of incorporating meteorological predictions in irrigation scheduling to reduce uncertainty.

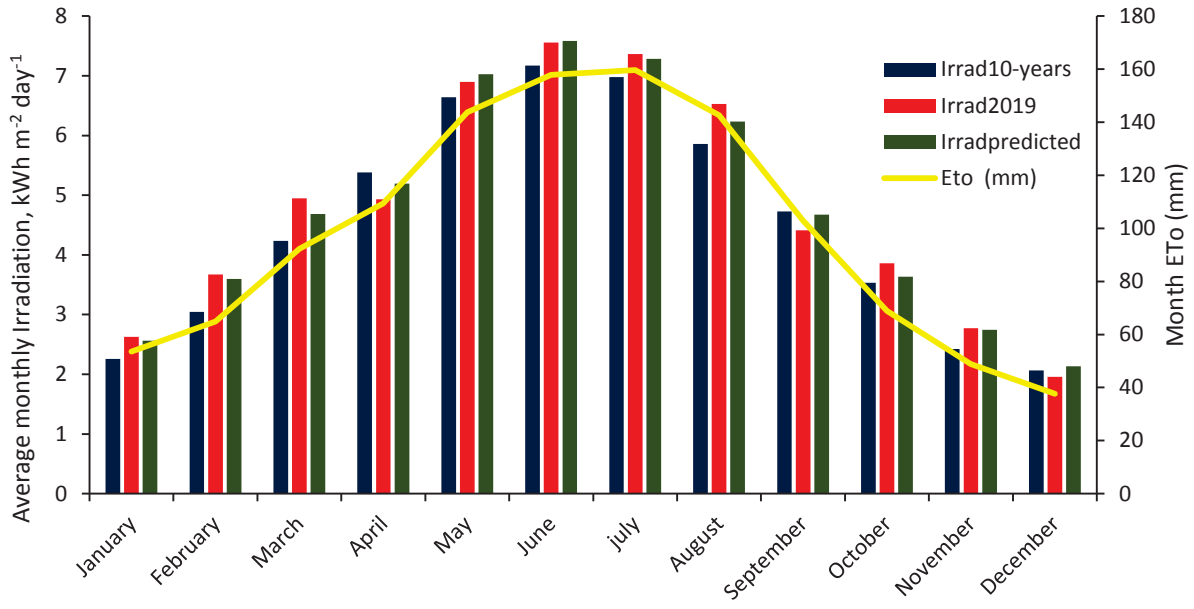

Fig.10. $Irrad_{10\text{-}years}$ (blue), $Irrad_{predicted}$ (green) y $Irrad_{2019}$ (red) monthly mean in kW $m^{-2}day^{-1}$, monthly ETo of the study area (mm) (yellow).

The irradiance and temperature, and with it the $Pnet_{d,h}$, were established every Monday of 2019, both for the parameters predicted by weather predictions (SCE1, SCE3), as for the predictions made using the average data from the last 10 years (SCE2, SCE4). As can be seen in Table 3, the daily relative errors of irradiance, temperature and Pnet were analysed for the period of maximum IN (from April 1st to September 30th), for the periods of minimum IN (from January 1st to March 31st and from October 1st to December 31st), and for the entire year 2019, as well as the maximum and minimum relative error and the percentage standard deviation produced.

Table 3.

Analysis of daily temperature, irradiance and Pnet (%) errors for the periods of maximum IN, minimum IN and for the rest of the year.

	Temperature		Irradiance		Pnet	
	Predicted data	Historical data	Predicted data	Historical data	Predicted data	Historical data
Square error at time of maximum IN (%)	5,1	7,3	28,5	55,0	26,3	50,0
Square error at time of minimum IN (%)	10,4	20,1	23,1	45,1	21,7	42,0
Annual Square error (%)	7,8	13,7	25,8	50,0	24,0	46,0
Minimum error (%)	0,0	0,1	0,0	0,4	0,1	0,1
Typical deviation (%)	8,4	16,2	75,3	157,0	70,3	143,8

Upon conducting a study that compares the Pnet based on the average data from the last 10 years (SCE 2, SCE 4), and the Pnet calculated using weather predictions data (SCE 1, SCE 3) respectively against the Pnet using actual data measured in the year 2019, the variation of Pnet can be seen throughout 2019. The observed error was improved to 24% when using our proposed methodology with the predicted values, as opposed to 42% when using the historical data. Figure 11 shows the Pnet predicted using weather forecasts, after applying the Kalman filter, the Pnet based on historical data and the Pnet calculated with data measured in 2019.

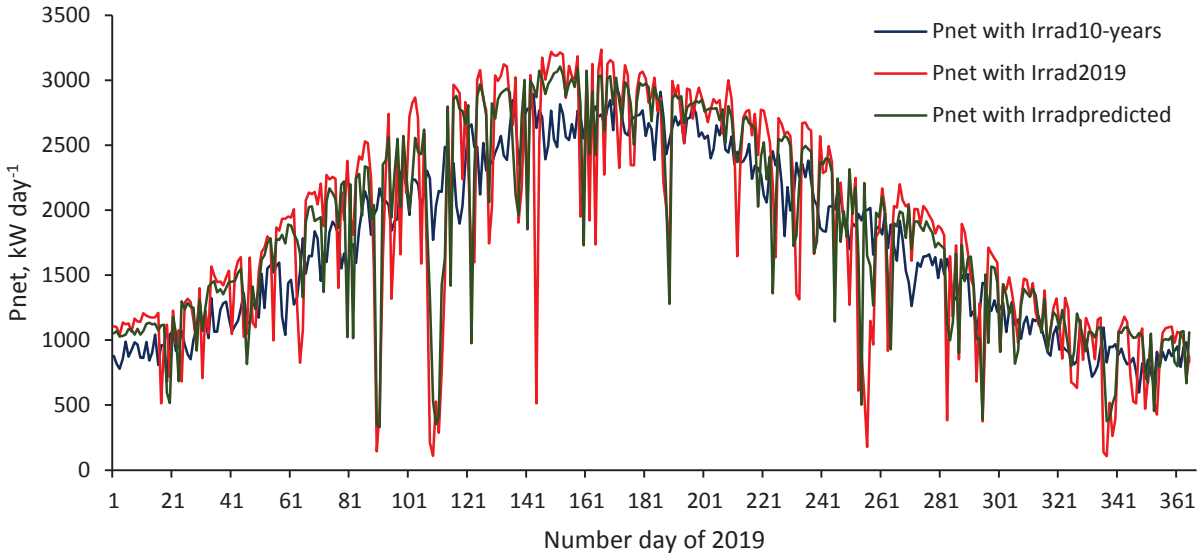

Fig.11. Pnet in kW day^{-1} of 2019 (red), Pnet predicted in kW day^{-1} using the mean of 10-year data (blue) and Pnet predicted in kW day^{-1} using meteorological predictions (green).

To demonstrate the importance of the configuration of the irrigation sectors, the 23rd June, 2019, a day without clouds, has been chosen. Figure 12 shows the $Irrad_{predicted}$, $Irrad_{10\text{-}years}$ and $Irrad_{2019}$ for that day, as well as the minimum irradiance required to make the network operate on PV power for each of the sectors that make up the network.

It is observed that the sectors were only operational between the irradiances 265 and 330 Wm^{-2}, and did not make use of the energy that was less than 265 Wm^{-2} or greater than 330 Wm^{-2}. Therefore, methodologies should be established in order to take advantage of all the PV energy throughout the day such as that proposed by (Mérida García et al., 2018; Zavala et al., 2020) where the simultaneous operation of several irrigation sectors reduces the cost of the PV system, making it advantageous in terms of Energy Use Efficiency. Another option is to study the possibility of establishing dynamic sectors with different $Pmin_i$ that better adjust to the irradiance available there by optimizing the use of PV energy.

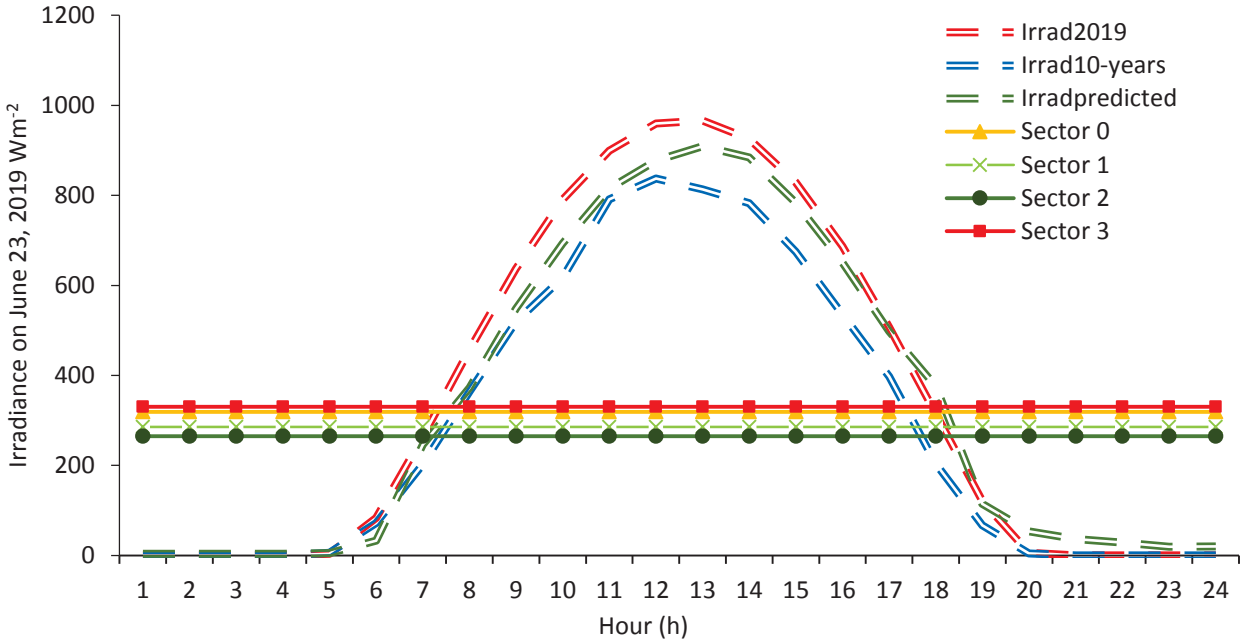

Fig. 12. Irradiance measured in 2019 (Wm^{-2}) (red), mean predicted irradiance of the last 10 years (Wm^{-2}) (blue), irradiance predicted by meteorological predictions (Wm^{-2}) (green) and irradiance minimum to reach the required power of each sector.

3.2. Evaluation of the programming of the operation of the irrigation network

This section studies how irrigation programming based on predictions affected the differential use of PV and conventional energy. The evaluation of the irrigation schedule for each sector was carried out by analysing the following factors: the irrigation and drainage doses, the irrigation hours carried out respectively by conventional energy and PV energy and the soil moisture for the 4 sectors. IT_{min} was set to 0.5 h to avoid excessive system start-ups and shutdowns.

The target humidity was set at the FCi (110 mm) and the point of minimum humidity was established as 25% lower than the FCi, that is, 82.5 mm. Drainage occurred when there was precipitation, since the possibility that soil moisture exceeded the field capacity only existed when there was rain, as described in equations 8 and 9.

To avoid the problem of drainage due to rainfall, in future works rainfall predictions should be improved and implemented (An-Vo et al., 2019) especially using a wider temporal framework.

3.2.1. Evaluation of irrigation dose and drainage.

Each sector was irrigated depending on its proximity to the target humidity (i.e. FC_i, or $W_{crit,I}$, of the ETc) determined for that week, the rainfall and the hours of available PV energy. As for $ITacu_i$, this could be less than IT_{std} or $ITPred_{week}$ of the one already established, because it would be lower if there were irrigations lower than IT_{min}, or if the CC_i was exceeded. On the contrary, a particular week's irrigation dose would increase if soil moisture fell below the minimum set threshold, which was 25% of the FC_i.

Fig 13 shows the annual irrigation dose for each sector depending on each of the scenarios. The annual consumptions for the 4 sectors were 2853.6 mm, 2869 mm, 2877.2 mm and 2897 mm for scenarios SCE1, SCE2, SCE3 and SCE4 respectively, showing that the least amount of irrigated water was achieved when using the combination of ETc $_{Predicted}$ and $Irrad_{predicted}$ (SCE1).

Drainage in the case study did not occur due to irrigation since the latter was halted once the target humidity (FC_i) was reached. However, in the periods when precipitation occurred, drainage was dependent on the proximity of the target moisture to the soil moisture. In periods of precipitation when the target moisture was reached, the drainage was equal to the precipitation, while the closer the soil moisture was to the minimum moisture permitted the more capacity the soil had to retain precipitated water.

Fig 13 shows the annual drainage for the 4 sectors depending on each of the scenarios. Annual drainage was 700.6 mm, 716 mm, 721.3 mm and 719.2 mm for scenarios SCE 1, SCE2, SCE3 and SCE4 respectively, showing that the least amount of drainage water was obtained when combining ETc $_{Predicted}$ and $Irrad_{predicted}$ (SCE1).

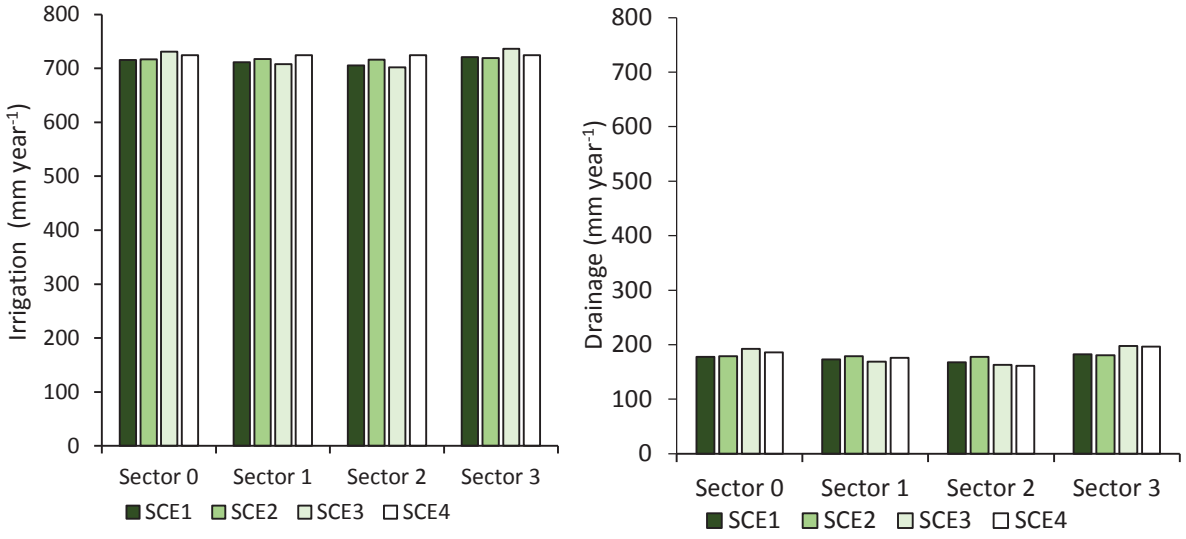

Fig. 13. mm of irrigation and mm of drainage per sector according to the different SEC1, SCE2, SCE3 and SCE4 scenarios.

3.2.2. Evaluation of sectors

3.2.2.1. Evaluation of sectors for the use of photovoltaic energy

The total annual operating hours employed irrigating the 4 sectors were 1698.5h, 1707.7h, 1712.6 and 1710.2h for scenarios SCE 1, SCE2, SCE3 and SCE4 respectively, showing that the least need for operating hours occurred when using the combination of $ETc_{Predicted}$ and $Irrad_{predicted}$ (SCE1).

Figure 14 shows the irrigation hours powered by PV energy and conventional energy respectively in separate diagrams. The sum of the two is the total hours of irrigation that had to be employed over the course of a year to cover the irrigation needs that had been established.

The sector that required the fewest hours of conventional energy was the one with the highest $Pmin_i$ and so on successively until reaching the sector with the lowest $Pmin_i$. Reciprocally, the sector which received the most hours of PV energy was also the one with the highest $Pmin_i$, the other sectors following consecutively from highest to lowest $Pmin_i$.

The annual PV hours supplying irrigation to the 4 sectors were 1322.6h, 1236h, 1257.1h and 1144.6h for scenarios SCE 1, SCE2, SCE3 and SCE4 respectively, showing that the highest use of PV energy irrigation hours was when using the combination of $ETc_{Predicted}$ and $Irrad_{predicted}$ (SCE1). Alternatively, the annual hours using conventional energy to supply irrigation to the 4 sectors were 375.9h, 471.8h, 455.6h and 565.7h for scenarios SCE 1, SCE2, SCE3 and SCE4 respectively, showing that the lowest use of conventional energy irrigation hours happened when combining $ETc_{Predicted}$ and $Irrad_{predicted}$ (SCE1).

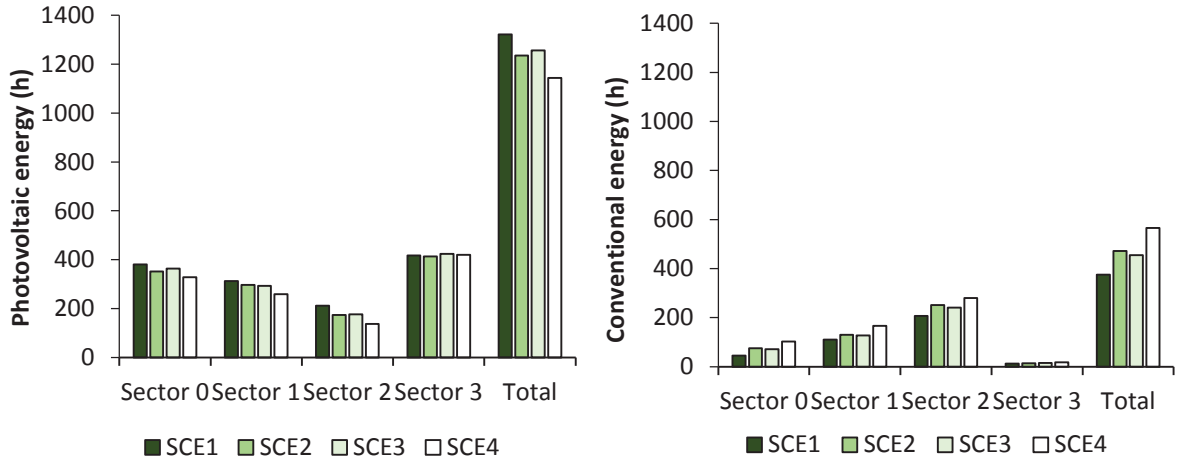

Fig. 14. Hours of irrigation by PV energy and hours of irrigation by conventional energy by sectors according to the different scenarios SEC1, SCE2, SCE3 and SCE4. Percentage data appear in Table 4.

Conventional energy was connected on those occasions when the irradiance was not sufficient to perform the irrigation already programmed by means of the predictions of both $Irrad_{predicted}$ and $Irrad_{10\text{-}years}$. On the other hand, conventional energy was also connected at those times when the soil moisture was less than 25% of the target humidity (FC_i) and there

was no PV energy available to supply the system, as indicated in Figure 15. Here we can observe that the hours of irrigation when conventional energy was used in the SCE1 and SCE2 scenarios was due to the fact that the humidity had dropped below 25% of the FCi. However, for the SCE3 and SCE4 scenarios the use of conventional energy was mainly due to errors in weather forecasting.

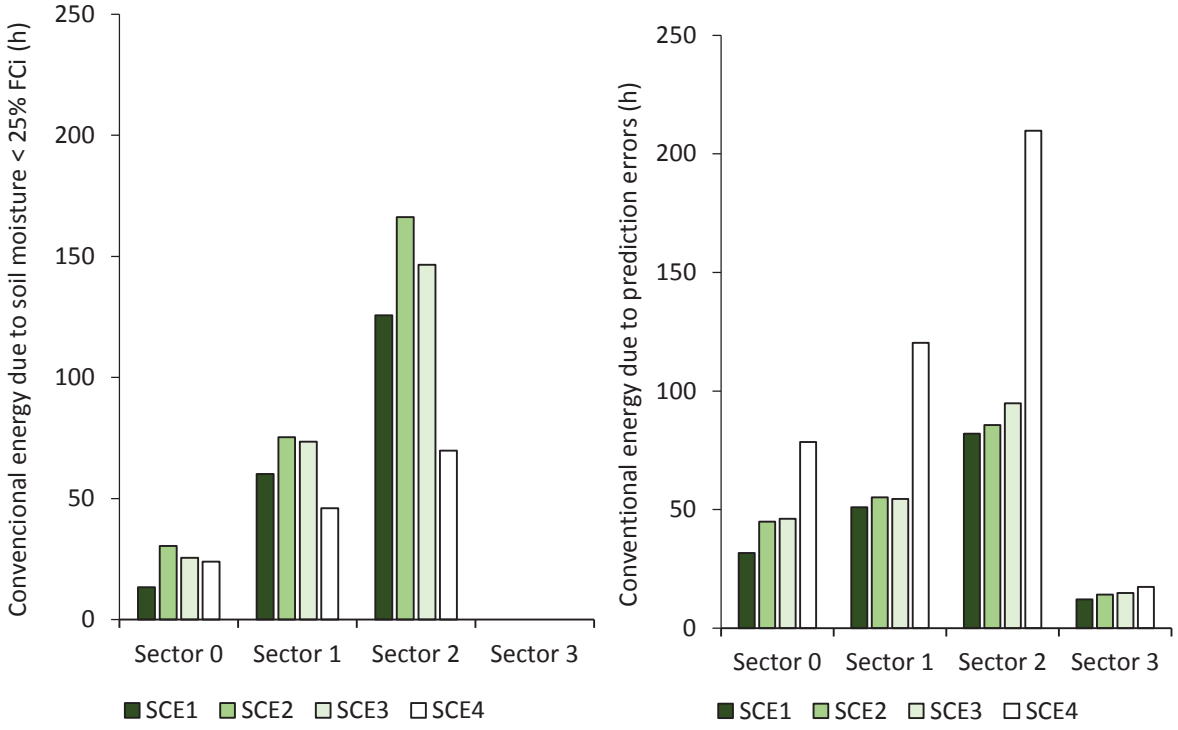

Fig. 15. Hours of irrigation using conventional energy due to soil humidity being less than 25% of the FCi or due to errors in the irrigation programming by sectors according to the different SEC1, SCE2, SCE3 and SCE4 scenarios.

Taking into account that the power system was a mixed one, where both PV and conventional energies were used, an analysis of the absolute error made using the predictions of $Irrad_{10\text{-}years}$ and $Irrad_{predicted}$ compared to the $Irrad_{2019}$ respectively, was carried out. This was achieved by analysing the differences between the average values of measured and predicted irradiance for each hour of the day during the year of 2019. In this way, taking into account the times when the greatest absolute positive error occurred between the measured and predicted irradiance, the conventional electricity consumption could be estimated, since these hours coincided on average with when the predicted irradiances were less than the $Irrad_{2019}$ ones. However, the $Pmin_i$ would have to be guaranteed at least for the hours when the equipment operated on PV energy, in the case of irradiance variation. When irrigation took place in the event that the humidity dropped below 25% of the FC_i, these irrigations could be carried out in the off-peak hours of lowest cost.

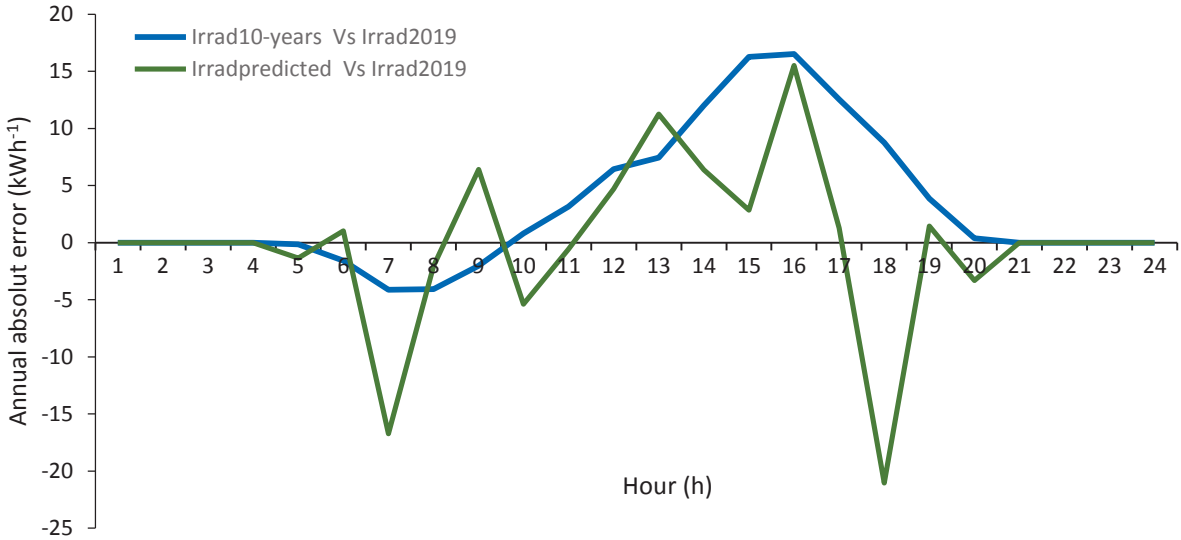

Fig. 16. Absolute error in kW for the irradiance predicted by meteorological data (green) and the irradiance predicted with mean data from the last 10 years (blue), compared to the irradiance measured in 2019.

The percentages between the hours of irrigation performed using PV energy and the hours of available energy are 13.37%, 12.52%, 12.74% and 11.64% for scenarios SCE1, SCE2, SCE3 and SCE4 respectively. From this it can be observed that the greatest uses of PV energy occurred in scenarios SCE1 and SCE3 where $Irrad_{predicted}$ was used. Researchers in (Zavala et al., 2020) managed to go from 15.4 % to 18.4 % through a process of combining the sectors. The aforementioned scenarios used 79% and 75% of PV energy respectively compared to scenarios SCE2 and SC4 which used 74% and 68% PV energy respectively.

In Table 4 the total number of irrigation hours for each scenario and for each sector are described. In addition, the percentages of the total irrigation time conducted with renewable energies for each of the sectors and scenarios are also indicated. The difference between the total hours of irrigation and the hours irrigated by renewable energies allows us to obtain the percentages of hours of irrigation supplied by conventional energy for each of the sectors and scenarios.

Table 4 shows the percentage of hours irrigated with conventional energy for these two situations.

Table 4.

Total hours of irrigation time (IT), total kWh, % of hours of irrigation by PV energy, % of hours of conventional energy and% of hours of irrigation by conventional energy due to soil moisture or prediction error.

Total IT (h)	Sector 0	Sector 1	Sector 2	Sector 3
SCE1	426,1	423,4	420,0	429,1
SCE2	426,7	426,9	426,1	427,9
SCE3	435,2	421,4	417,9	438,2
SCE4	431,1	425,2	416,4	437,5

Total energy (kWh)	Sector 0	Sector 1	Sector 2	Sector 3
SCE1	54.791,0	48.948,6	45.192,4	56.977,9
SCE2	54.879,2	49.349,8	45.852,8	56.830,8
SCE3	55.964,6	48.709,2	44.970,4	58.186,4
SCE4	55.439,1	49.151,5	44.808,0	58.104,3

IT with PV energy (%)	Sector 0	Sector 1	Sector 2	Sector 3
SCE1	89,4	73,8	50,6	97,2
SCE2	82,3	69,4	40,9	96,7
SCE3	83,5	69,7	42,3	96,6
SCE4	76,2	60,9	32,9	96,0

IT with conventional energy (%)	Sector 0	Sector 1	Sector 2	Sector 3
SCE1	10,6	26,2	49,4	2,8
SCE2	17,7	30,6	59,1	3,3
SCE3	16,5	30,3	57,7	3,4
SCE4	23,8	39,1	67,1	4,0

IT conventional energy (%) due to 25% of FCi.	Sector 0	Sector 1	Sector 2	Sector 3
SCE1	29,5	54,1	60,5	0,0
SCE2	40,4	57,7	66,0	0,0
SCE3	35,6	57,4	60,7	0,0
SCE4	23,3	27,6	25,0	0,0

IT conventional energy due to prediction error (%)	Sector 0	Sector 1	Sector 2	Sector 3
SCE1	70,5	45,9	39,5	100,0
SCE2	59,6	42,3	34,0	100,0
SCE3	64,4	42,6	39,3	100,0
SCE4	76,7	72,4	75,0	100,0

As sector 3 was the first to be assigned $Pnet_{d,h}$, it obtained a higher percentage of PV energy and it was not necessary to use conventional energy to maintain this sector´s humidity level above $W_{crit,i}$. Only prediction errors forced the use of conventional energy. On the other hand, sector 2, the sector with the lowest $Pmin_i$, was the one that made the greatest use of conventional energy and the largest percentage of it was due to the fact that $W_{crit,i}$ was not reached.

Once the causes of the PV power failure have been determined, the next step would be to study which is the appropriate alternative energy to cover this gap. Investigators (Pardo et al., 2019) studied the effect of incorporating batteries for storing energy to protect the system against emergencies, and the results showed that there is no universal solution. This is due to the fact that there are a large number of alternatives available when buying the equipment and hence in future savings. (Mérida García et al., 2019) demonstrated from an environmental point of view that PV energy was the lowest cost option both when connected to the grid, as

when not, compared to using generator sets. Moreover, the possibility of exporting excess energy to the electricity grid resulted in six times less environmental impact compared to an installation that was not connected.

4. Conclusions

Photovoltaic energy has been applied to very different types of irrigation systems depending on: the type of delivery method employed, that is, by gravity from a reservoir or by direct injection; or the type of electricity supply, that is, connected to the electrical grid or isolated from it.

Most of the direct injection systems that have been applied consist of a limited number of hydrants that are arranged into sectors. In the cases where the photovoltaic installation is off-grid, if there are disturbances in the irradiance, the system stops working unless there are auxiliary systems such as batteries or generator sets.

In networks of a certain magnitude with a large number of hydrants which can have multi-emitters, the commands for opening and closing the irrigation outlets and for activating and stopping the pumping groups must be correctly programmed in advance so as to guarantee the optimum functioning of the system and avoid unwanted transient phenomena.

The use of short-term meteorological predictions, using a week´s timeframe, allows the estimation of the irradiance and the irrigation needs of the crops with greater precision, permitting irrigation operations to be programmed in advance. However, every prediction is subject to some uncertainty, and if the prediction is not met an additional energy source is needed. In this case study, the relative error in the estimation of net power incurred during the period of greatest irrigation needs was 26.3% for weather forecasts, as opposed to 50% using historical data.

The application of weather forecasts in the calculation of irradiance and irrigation needs (SCE1) as opposed to the use of historical data and the calculation of evapotranspiration based on what happened in the past (SCE4) led to an improved use of renewable energy from 68.7% to 79.3%, and to an increase in the use of available photovoltaic energy from 11.64% to 13.37%.

To improve this last indicator, we must act on the irrigation programming by designing dynamic sectors whose minimum power of each sector is adapted along the net power.

Improving the predictions, accompanied by a reduction in the prediction timeframe, will improve the percentage of renewable energy used and increase the hours of available energy use while keeping the moisture levels within requirements.

References

Adamsab, K., Saif, M., Saif, S., Khamis, I., Talib, W., 2020. Hybrid powered intelligent irrigation system using Oman Falaj and solar energy. Mater. Today Proc. https://doi.org/10.1016/j.matpr.2020.09.033

Albertos, P., Sala, A., 2004. El control borroso, una metodología integradora. RIAI - Rev. Iberoam. Automática e Informática Ind. 2(1), 22–31.

Allen, R.G., Pereira, L.S., Raes, D., Smith, M., 1998. Crop evapotranspiration guide- lines for computing crop water requirements. Irrigation and Drainage. FAO 56.300.

An-Vo, D.A., Mushtaq, S., Reardon-Smith, K., Kouadio, L., Attard, S., Cobon, D., Stone, R., 2019. Value of seasonal forecasting for sugarcane farm irrigation planning. Eur. J. Agron. 104, 37–48. https://doi.org/10.1016/j.eja.2019.01.005

Bakelli, Y., Hadj Arab, A., Azoui, B., 2011. Optimal sizing of photovoltaic pumping system with water tank storage using LPSP concept. Sol. Energy 85, 288–294. https://doi.org/10.1016/j.solener.2010.11.023

Caldera, U., Breyer, C., 2019. Assessing the potential for renewable energy powered desalination for the global irrigation sector. Sci. Total Environ. 694, 133598. https://doi.org/10.1016/j.scitotenv.2019.133598

Carricondo-Anton, J.M., Jiménez-Bello, M., Martínez Alzamora, F., Sala, A., 2019. Análisis de las Predicciones Climáticas a partir de distintos Servicios Climáticos para la Programación del Riego. XXXVII Congr. Nac. Riegos.

Castel, J.., 2000. Water use of developing citrus canopies in Valencia. Proceeding Int. Soc. Citric. IX Congres, 223–226.

Díaz, J.A.R., Montesinos, P., Poyato, E.C., 2012. Detecting Critical Points in On-Demand Irrigation Pressurized Networks - A New Methodology. Water Resour. Manag. 26, 1693–1713. https://doi.org/10.1007/s11269-012-9981-8

Dorado, J., Ruíz, F.J., 2018. Implementación de filtros de Kalman como método de ajuste a los modelos de pronóstico (GFS) de temperaturas máximas y mínima para algunas ciudades de Colombia. Grup. Model. Tiempo y Clima. Subdirección Meteorol. – IDEAM.

El-houari, H., Allouhi, A., Rehman, S., Buker, M.S., Kousksou, T., Jamil, A., El Amrani, B., 2020. Feasibility evaluation of a hybrid renewable power generation system for sustainable electricity supply in a Moroccan remote site. J. Clean. Prod. 277, 123534. https://doi.org/10.1016/j.jclepro.2020.123534

Elkadeem, M.R., Wang, S., Sharshir, S.W., Atia, E.G., 2019. Feasibility analysis and techno-economic design of grid-isolated hybrid renewable energy system for electrification of agriculture and irrigation area: A case study in Dongola, Sudan. Energy Convers. Manag. 196, 1453–1478. https://doi.org/10.1016/j.enconman.2019.06.085

Espinosa-Tasón, J., Berbel, J., Gutiérrez-Martín, C., 2020. Energized water: Evolution of water-energy nexus in the Spanish irrigated agriculture, 1950–2017. Agric. Water Manag. 233, 106073. https://doi.org/10.1016/j.agwat.2020.106073

Evensen, G., 2003. The Ensemble Kalman Filter: theoretical formulation and practical implementation. Ocean Dyn. 53, 343–367. https://doi.org/10.1007/s10236-003-0036-9

Fernández García, I., Rodríguez Díaz, J.A., Camacho Poyato, E., Montesinos, P., 2013. Optimal

Operation of Pressurized Irrigation Networks with Several Supply Sources. Water Resour. Manag. 27, 2855–2869. https://doi.org/10.1007/s11269-013-0319-y

García Morillo, J., McNabola, A., Camacho, E., Montesinos, P., Rodríguez Díaz, J.A., 2018. Hydro-power energy recovery in pressurized irrigation networks: A case study of an Irrigation District in the South of Spain. Agric. Water Manag. 204, 17–27. https://doi.org/10.1016/j.agwat.2018.03.035

Generalitat Valenciana, 2020. Estrategia Valenciana de Regadíos.

GIZ, 2016. Frequently Asked Questions may Powered Solar Irrigation Pumps.

González Perea, R., Camacho Poyato, E., Montesinos, P., Rodríguez Díaz, J.A., 2014. Critical points: Interactions between on-farm irrigation systems and water distribution network. Irrig. Sci. 32, 255–265. https://doi.org/10.1007/s00271-014-0428-2

Hamidat, A., Benyoucef, B., Hartani, T., 2003. Small-scale irrigation with photovoltaic water pumping system in Sahara regions. Renew. Energy 28, 1081–1096. https://doi.org/10.1016/S0960-1481(02)00058-7

Han, X., Franssen, H.J.H., Montzka, C., Vereecken, H., 2014. Soil moisture and soil properties estimation in the Community Land Model with synthetic brightness temperature observations. Water Resour. Res. 50, 6081–6105. https://doi.org/10.1002/2013WR014586

Hunt, B.R., Kostelich, E.J., Szunyogh, I., 2007. Efficient data assimilation for spatiotemporal chaos: A local ensemble transform Kalman filter. Phys. D Nonlinear Phenom. 230, 112–126. https://doi.org/10.1016/j.physd.2006.11.008

Jiménez-Bello, M.A., Martínez Alzamora, F., Bou Soler, V., Ayala, H.J.B., 2010. Methodology for grouping intakes of pressurised irrigation networks into sectors to minimise energy consumption. Biosyst. Eng. 105, 429–438. https://doi.org/10.1016/j.biosystemseng.2009.12.014

Kalman, R., 1960. A New Approach to Linear Filtering and Prediction Problems. Trans. ASME - J. basic Eng. 82, 35–45. https://doi.org/10.1115/1.3662552

Li, D., Hendricks Franssen, H.J., Han, X., Jiménez-Bello, M.A., Martínez Alzamora, F., Vereecken, H., 2018. Evaluation of an operational real-time irrigation scheduling scheme for drip irrigated citrus fields in Picassent, Spain. Agric. Water Manag. 208, 465–477. https://doi.org/10.1016/j.agwat.2018.06.022

Li, J., Li, L., Wang, H., Ferentinos, K.P., Li, M., Sigrimis, N., 2017. Proactive energy management of solar greenhouses with risk assessment to enhance smart specialisation in China. Biosyst. Eng. 158, 10–22. https://doi.org/10.1016/j.biosystemseng.2017.03.007

Lian, J., Zhang, Y., Ma, C., Yang, Y., Chaima, E., 2019. A review on recent sizing methodologies of hybrid renewable energy systems. Energy Convers. Manag. 199, 112027. https://doi.org/10.1016/j.enconman.2019.112027

López-Luque, R., Reca, J., Martínez, J., 2015. Optimal design of a standalone direct pumping photovoltaic system for deficit irrigation of olive orchards. Appl. Energy 149, 13–23. https://doi.org/10.1016/j.apenergy.2015.03.107

Lorite, I.J., Ramírez-Cuesta, J.M., Cruz-Blanco, M., Santos, C., 2015. Using weather forecast data for irrigation scheduling under semi-arid conditions. Irrig. Sci. 33, 411–427. https://doi.org/10.1007/s00271-015-0478-0

MAPAMA, 2002. Ministerio de Agricultura, Pesca y Alimentación. [WWW Document]. «BOE» núm.

101, 27 abril 2002. URL https://www.boe.es/buscar/pdf/2002/BOE-A-2002-8129-consolidado.pdf (accessed 8.12.20).

Markvart, T., Castaner, L., 2003. Practical Handbook of Photovoltaics: Fundamentals and Applications, Practical Handbook of Photovoltaics: Fundamentals and Applications. Elsevier Science & Technology, Kidlington.

MARM, 2010. Estrategia Nacional Para La Modernización Sostenible De Los Regadios H2015 [WWW Document]. Dir. Gen. del Agua. URL https://www.miteco.gob.es/images/es/2ISA_EAE_ENMSRH2015_210710_parte1_tcm30-183585.pdf (accessed 8.12.20).

Martínez-Gimeno, M., Jiménez-Bello, M., Lidón, A., Manzano, J., Badal, E., Pérez-Pérez, J., Bonet Perez de León, L., Intrigliolo, D., Esteban Hernandiz, A., 2018. Mandarin irrigation scheduling by means of frequency domain reflectometry soil moisture monitoring. Agric. Water Manag. 235, 106–151. https://doi.org/10.1016/j.agwat.2020.106151

Meah, K., Ula, S., Barrett, S., 2008. Solar photovoltaic water pumping-opportunities and challenges. Renew. Sustain. Energy Rev. 12, 1162–1175. https://doi.org/10.1016/j.rser.2006.10.020

Mérida García, A., Fernández García, I., Camacho Poyato, E., Montesinos Barrios, P., Rodríguez Díaz, J.A., 2018. Coupling irrigation scheduling with solar energy production in a smart irrigation management system. J. Clean. Prod. 175, 670–682. https://doi.org/10.1016/j.jclepro.2017.12.093

Mérida García, A., Gallagher, J., McNabola, A., Camacho Poyato, E., Montesinos Barrios, P., Rodríguez Díaz, J.A., 2019. Comparing the environmental and economic impacts of on- or off-grid solar photovoltaics with traditional energy sources for rural irrigation systems. Renew. Energy 140, 895–904. https://doi.org/10.1016/j.renene.2019.03.122

Milano, M., Ruelland, D., Fernandez, S., Dezetter, A., Fabre, J., Servat, E., Fritsch, J.M., Ardoin-Bardin, S., Thivet, G., 2013. Current state of Mediterranean water resources and future trends under climatic and anthropogenic changes. Hydrol. Sci. J. 58, 498–518. https://doi.org/10.1080/02626667.2013.774458

Moreno, M.A., Carrión, P.A., Planells, P., Ortega, J.F., Tarjuelo, J.M., 2007. Measurement and improvement of the energy efficiency at pumping stations. Biosyst. Eng. 98, 479–486. https://doi.org/10.1016/j.biosystemseng.2007.09.005

Pardo, M.Á., Manzano, J., Valdes-Abellan, J., Cobacho, R., 2019. Standalone direct pumping photovoltaic system or energy storage in batteries for supplying irrigation networks. Cost analysis. Sci. Total Environ. 673, 821–830. https://doi.org/10.1016/j.scitotenv.2019.04.050

Powell, J. W., Welsh, J.M., Farquharson, R., 2019. Investment analysis of solar energy in a hybrid diesel irrigation pumping system in New South Wales, Australia. J. Clean. Prod. 224, 444–454. https://doi.org/10.1016/j.jclepro.2019.03.071

Powell, Janine W., Welsh, J.M., Pannell, D., Kingwell, R., 2019. Can applying renewable energy for Australian sugarcane irrigation reduce energy cost and environmental impacts? A case study approach. J. Clean. Prod. 240, 118177. https://doi.org/10.1016/j.jclepro.2019.118177

Raes, D., 1982. A summary simulation model of the water budget of a cropped soil, Leuven Uni. ed, Dissertationes de Agricultura n° 122.K.U. Leuven, Belgium.

Raes, D., Geerts, S., Kipkorir, E., Wellens, J., Sahli, A., 2006. Simulation of yield decline as a result of water stress with a robust soil water balance model. Agric. Water Manag. 81, 335–357. https://doi.org/10.1016/j.agwat.2005.04.006

Raes, D., H. Lemmens, P., Van Aelst, M., Bulcke, V., Smith, M., 1988. IRSIS – Irrigation scheduling information system. Dep. Land Management, Reference Manual 3.

Santra, P., Meena, H.M., Yadav, O.P., 2021. Spatial and temporal variation of photosynthetic photon flux density within agrivoltaic system in hot arid region of India. Biosyst. Eng. 209, 74–93. https://doi.org/10.1016/j.biosystemseng.2021.06.017

Turral, H., Burke, J., Faures, J.., 2011. Climate Change, Water and Food Security. Rome. https://doi.org/10.16309/j.cnki.issn.1007-1776.2003.03.004

UN DESA, 2019. World Population Prospects 2019, Department of Economic and Social Affairs. World Population Prospects 2019. United Nations, Department of Economic and Social Affairs, New York, USA.

van Mourik, S., van Beveren, P.J.M., López-Cruz, I.L., van Henten, E.J., 2019. Improving climate monitoring in greenhouse cultivation via model based filtering. Biosyst. Eng. 181, 40–51. https://doi.org/10.1016/j.biosystemseng.2019.03.001

Zavala, V., López-Luque, R., Reca, J., Martínez, J., Lao, M.T., 2020. Optimal management of a multisector standalone direct pumping photovoltaic irrigation system. Appl. Energy 260, 114261. https://doi.org/10.1016/j.apenergy.2019.114261